Investigate the Shore, Sound out the Past: Methods and Practices of Maritime Prehistory
Explorer la côte, sonder le passé : méthodes et pratiques de la préhistoire maritime
Actes de la séance de la Société préhistorique française de Brest (décembre 2020)
Textes publiés sous la direction de Grégor Marchand (†), Yvan Pailler et Pierre Stéphan
Paris, Société préhistorique française, 2023
(Séances de la Société préhistorique française, 19), p. 19-44
www.prehistoire.org
ISSN : 2263-3847 – ISBN : 978-2-913745-92-6

Potential and Limitations of Geomagnetic Prospecting for the Imaging of Prehistoric Sites in Coastal Areas: a Case Study of the Port Neuf Site (Hoedic)

Potentiels et limites de la prospection géomagnétique appliquée à l'imagerie de sites préhistoriques en zone côtière : le site de Port Neuf (Hoedic)

Francois Lévêque, Grégor Marchand (†), Martin Moucheron, Luis Teira, Pablo Arias

Abstract: Through a case study of the coastal Mesolithic site of Port Neuf (Hoedic), this article aims to introduce archaeologists to the use of geomagnetic prospection methods in the context of irregular vegetation cover and topography inherent to this type of coastal site. The constraints and limitations of the method are discussed, e.g. the negative influence of pollution by a large metal mass on the information obtained. The data processing carried out to attenuate the disturbance induced by this magnetic pollution does not allow relevant information to be extracted over the entire polluted area. It is also shown that in the context of the presence of dune cover, such as that covering the archaeological levels, it is necessary to study the variation in magnetic field intensity rather than its vertical gradient by gradiometry. The use of other complementary geophysical methods provides information to refine the proposed interpretations, particularly concerning the presence of hearths. For example, electromagnetic methods, such as the use of conductivity meters, provide information on the spatial variation of the substrate's capacity to conduct electricity or a magnetic field at the site scale, or the use of contact sensors, which at the scale of the excavation help to determine areas of potential hearths by detecting zones of magnetic enhancement. The need for archaeologists and geophysicists to work together and for excavators to adopt these tools is discussed.
Keywords: Geomagnetic prospection, coastal archaeology, hearth, Armorique, magnetic susceptibility, Hoedic.

Résumé : Les sites archéologiques littoraux constituent des objets pour lesquels le recours aux méthodes géophysiques est pertinent, que ce soit avant d'entreprendre des fouilles ou au cours de leur réalisation. L'utilisation du feu par les sociétés préhistoriques est la source de thermoaltérations des phases minéralogiques riches en fer, qui sont produites par l'élévation de température des matériaux, à partir de températures de l'ordre de 200 à 250 °C. Ces transformations produisent un enrichissement en minéraux magnétiques. De plus, l'élévation de température engendre une augmentation de l'ordre magnétique de ces minéraux qui vont avoir tendance à acquérir une aimantation dans la direction du champ magnétique ambiant lors de leur refroidissement. Les méthodes magnétiques sont, de ce fait, des outils privilégiés pour étudier les sites archéologiques préhistoriques. Ces enrichissements magnétiques et les aimantations thermorémanentes acquises lors du dernier refroidissement des matériaux sont la source d'anomalies locales du champ magnétique. La prospection géomagnétique a pour objet de cartographier ces anomalies. Grâce aux cadences de mesures élevées des magnétomètres, plus de dix mesures par seconde, la prospection géomagnétique est une méthode performante pour obtenir une information de résolution spatiale élevée en un temps d'acquisition limité. Les enrichissements magnétiques peuvent aussi être détectés par la réalisation de mesures de susceptibilité ou de viscosité magnétique avec des capteurs de contact, directement sur les matériaux exposés à l'affleurement. Cet article se focalise sur la prospection géomagnétique et présente les prospections géophysiques réalisées sur le site mésolithique de Port Neuf (Hoedic) au titre d'exemple d'étude de site des îles armoricaines.
En contexte littoral, le couvert végétal et la topographie constituent des contraintes importantes pour la mise en œuvre d'une prospection géomagnétique. Afin d'obtenir une densité spatiale de mesures, régulière, à plusieurs dizaines de mesures par mètre carré, néces-

saire pour disposer d'une information de qualité suffisante, des repères visuels sont implantés tous les mètres. Un dispositif permet à l'opérateur de porter les deux capteurs du magnétomètre (GSMP35-G, GEM system) à une vingtaine de centimètres au-dessus de la surface du sol et à 25 cm de part et d'autre de l'axe d'avancée, permettant ainsi d'acquérir des profils de mesures tous les 50 cm.
La présence des vestiges d'un relais télégraphique est la source d'une anomalie magnétique majeure qui masque le signal archéologique recherché. La modélisation de cette anomalie par une équation mathématique permet de minimiser cette perturbation. Une information archéologique peut alors être extraite de la partie périphérique de l'anomalie majeure indésirable. La présence d'une couverture dunaire recouvrant les niveaux archéologiques éloigne les sources magnétiques potentielles de la surface de mesure. La mesure du gradient du champ magnétique (gradient vertical du champ magnétique ou pseudogradient de l'intensité du champ magnétique), classiquement mise en œuvre pour s'affranchir facilement de la variation temporelle du champ magnétique, n'est pas pertinente dans ce cas de figure à cause de l'éloignement des sources dont l'intensité est vraisemblablement modeste. Il est alors nécessaire de déterminer les variations d'intensité du champ magnétique. Pour éviter l'utilisation d'un second magnétomètre pour enregistrer en position fixe la variation temporelle du champ magnétique qui sera retranchée de l'enregistrement dynamique, celle-ci est estimée à l'aide d'une fonction polynomiale établie à partir de valeurs de mesures médianes de chaque profil aller-retour. Cette démarche permet de mettre en évidence des anomalies étalées spatialement mais d'intensité modeste, non visibles en gradiométrie. Ces anomalies constituent potentiellement les traces magnétiques de foyers enfouis sous la couverture dunaire. Afin d'affiner les interprétations de cette prospection géomagnétique, des prospections ont été menées avec un conductivimètre dans le secteur situé autour de la fouille effectuée par les époux Péquart dans les années 1930 (Péquart et Péquart, 1954). Les informations de conductivité électrique et de susceptibilité magnétique apparente apportées par ces dernières prospections sont décorrélées de l'information géomagnétique, ce qui est en faveur d'une source magnétique associée à une aimantation thermorémanante, de fait détectable uniquement par l'anomalie magnétique qu'elle crée.
La présence de coupes naturelles en bord de falaise et au niveau des sondages archéologiques a permis d'effectuer des relevés à l'aide d'un susceptibilimètre et d'un viscosimètre magnétique. Ces mesures révèlent la séquence de trois corps dunaires successifs, au niveau du sondage étudié, surmontant le niveau d'occupation mésolithique qui présente un fort enrichissement magnétique. Ces mesures de caractérisation des propriétés magnétiques des unités stratigraphiques sont complémentaires des autres prospections géophysiques. Réalisées au cours d'une fouille – d'abord par le géophysicien pour cerner la signification des variations constatées (variations qui dépendent fortement de la dynamique du fer dans les processus de pédoaltération), puis par le fouilleur en présence d'indices de feu, ou de manière systématique –, ces mesures permettraient de visualiser des objets invisibles à l'œil, sortes de « fantômes magnétiques », telles des soles de foyers dont la présence n'est pas trahie par des rubéfactions. L'existence d'un enrichissement magnétique dépend de la nature des matériaux chauffés. Un matériau dépourvu de fer ne sera pas impacté thermiquement du point de vue magnétique. En revanche, un fort enrichissement ne traduit pas systématiquement la présence de traces d'un foyer. Seule la caractérisation de la présence d'une aimantation thermorémanente, ou du moins de l'anomalie magnétique associée, est un gage de la présence d'un foyer. Pour réaliser cela, une prospection 3D à résolution infradécimétrique, comme celles réalisées dans les grottes préhistoriques (Burens et al., 2014 ; Grussenmeyer et al., 2014 ; Lévêque et Mathé, 2015, Jaubert et al., 2016), est envisageable. Cependant, cette démarche n'est pas concevable de manière systématique. L'alternative à une prospection 3D serait que les fouilleurs utilisent un gradiomètre magnétique miniature en complément d'un susceptibilimètre et/ou d'un viscosimètre. Un tel instrument n'existe pas sur le marché mais sa réalisation est tout à fait possible.
Mots-clés : prospection géomagnétique, archéologie littorale, foyer, Armorique, susceptibilité magnétique, Hoedic.

INTRODUCTION

The use of geophysical methods for the study of coastal prehistoric sites is on the increase (Bates et al., 2019; Napora et al., 2019; Giovas et al., 2020; Wilken et al., 2022), but identifying the best geophysical investigation approach is still an elusive goal as each case study has its own specificities. Indeed, the soil of each site will have its own particular physical characteristics and the nature, geometry and the depth of burial of the archaeological objects sought will differ. This article focuses on the use of magnetic methods and more specifically on the implementation of geomagnetic surveys. It provides a progress report on the evolution of the methods used on the coasts of the Armorican Massif (France) for several years (Cousseau et al., 2019; Duval et al., 2021; Pailler et al., 2022), the protocols being adapted to each new site according to the presumed specificities, access constraints (which may limit the technical means that can be applied) and to the archaeological problematic.

Although we are dealing with geomagnetic prospecting here, it is important to remember that the comparison of results obtained by several different geophysical methods is generally more informative than basing one's approach on a single method. Indeed, each method exploits different physical properties of the environment: mainly a site's capacity to sustain magnetisation and the presence of thermoremanent magnetisations (TRM), but also the capacity of the environment to propagate an electric current or electromagnetic wave. The same physical quantity may also be measured by instruments operating on different principles. Depending on the properties of the environment, significant differences can be observed due to differences in instrumental limits. For example, the study of variations in the magnetic properties of the environment can be addressed using (1) the spatial variation of the magnetic field through geomagnetic prospecting, which detects both variations in the magnetising capacity of the environment and the presence of permanent, mainly thermoremanent, magnetisations; (2) in a complementary way by measurements of magnetic susceptibility, a quantity that expresses the capacity of a material to carry a magnetisation, which is done by contact measurement with a kappameter on volumes smaller than a cubic decimeter; or (3) with a conductivity meter, which will determine variations in the so-called apparent magnetic susceptibility of the environment on much larger volumes, generally in cubic metre, varying according to the dimensions of the conductivity meter used.

A comprehensive presentation of all the geomagnetic surveys carried out in the Armorican coastal area in recent years is not feasible in this article. For this reason, this article will focus on a single representative site, the Mesolithic site of Port Neuf on the island of Hoedic (south Brittany, France). Before presenting this case study, we will first discuss the constraints of geomagnetic prospecting in the coastal context.

1. APPLICATION OF GEOMAGNETIC PROSPECTING TO THE IMAGING OF PREHISTORIC SITES IN COASTAL AREAS

1.1. Data acquisition

In near-surface geophysical imaging, whatever method is used, the spatial density of the measurements determines the accuracy of the observations that can be made. As magnetic field measurements do not require contact with the ground, they can be collected continuously, while moving. This and the high measurement rates of magnetometers (10 measurements per second or more) make geomagnetic prospecting a powerful method for obtaining high spatial resolution data in a limited measurement time. The usual type of area where the method is used is open land with an even surface and sparse vegetation, or after harvesting of arable crops. This is because, on the one hand, the absence of obstacles allows for movement along regularly spaced profiles and, on the other hand, the topographical effects on the deformation of the magnetic field are limited to those of the microreliefs generated by tillage. It is thus easy to obtain information at a regular spatial density of several tens of measurements per square metre over the surface of the surveyed area.

Apart from this high spatial resolution, however, the ability to image an object depends on there being a sufficient magnetic contrast between the surrounding materials and the object of interest. On a prehistoric site, the soil environment can be complex, and its magnetic properties can vary greatly. A sequence of paleosols may exist, marking phases of slowing down or non-deposition that favour pedogenesis. The present soil can form on various substrates: on the alterite of an ancient paleosurface, for example, if it has not been stripped by Quaternary erosion, or on a young substrate formed during the Holocene, such as alluvial deposits, coastal dune sands or bedrock brought to the surface by Quaternary erosion. As a general rule, a soil is more magnetic than the substrate on which it forms (Le Borgne, 1955; Fassbinder, 2015; Lévêque, 2021). However, the magnetic signature of a soil depends on its nature, specifically on the dynamics of iron in relation to those of organic matter. Its magnetisation capacity, classically assessed by magnetic susceptibility measurements, is strongly dependent on the amount of the most magnetic natural iron oxides it contains, namely the nanometric mineralogical phase of magnetite (Fe_3O_4) or its oxidized form maghemite (γ-Fe_2O_3). These substances, which are black and brown pigments, respectively, are inherently undetectable to the eye. Without a visual indicator, given the complexity of the generation of a soil's magnetic signature, it is difficult to estimate the magnetisation capacity of a soil without measuring its magnetic susceptibility.

An archaeological soil is generally more magnetic than a natural soil (Tite and Mullins, 1971), which can be explained by the addition of organic matter, compaction, clearing by burning, emptying of hearths, etc. Among influencing factors, the use of fire is of major interest for magnetic methods. Indeed, fire produces a thermo-alteration of the minerals present in its substrate. Depending on the redox conditions of the fire, iron-containing minerals can be the source of new magnetic particles. Thus, if the thermal wave, after evaporation of water (Brodard et al., 2016), exceeds 200-250°C, then magnetic minerals (known as ferrimagnetic minerals) are neoformed by the thermal action of fire on minerals containing iron in a weakly magnetic or non-magnetic form (known as canted antiferromagnetic and paramagnetic, respectively).

Thus, iron oxyhydroxides FeOOH (goethite, lepidocrocite) are dehydrated to form, depending on the oxidizing or reducing conditions of the gas phase, hematite (α-Fe_2O_3), maghemite (γ-Fe_2O_3) or magnetite (Fe_3O_4; Cudennec and Lecerf, 2004; Brodard et al., 2014). In the presence of carbon monoxide (CO), produced by partial fat burning for example, hematite can also be reduced to magnetite (Colombo et al., 1967; Yu et al., 2017), probably at temperatures below 400°C.

Besides the phenomenon of magnetic enhancement produced by thermo-alteration associated with fires, the magnetisation of the heated materials are heightened by this enhancement and by the magnetic order produced. The magnetic minerals originally present or neoformed, can carry, depending on their size, a permanent magnetisation, which is called thermoremanent. It is produced by the rise in temperature of the substrate to several hundred degrees Celsius. In addition to the thermo-alteration generated, this temperature frees the magnetic order of the magnetic minerals. During the cooling process, this magnetic order of these minerals is locked once again. The ambient geomagnetic field favours the alignment of magnetisations according to its direction, increasing the magnetic order.

This permanent magnetisation, called thermoremanent, thus fossilizes the past magnetic field. It is associated with a magnetisation induced by the interaction of the magnetisations of the magnetic minerals with the present geomagnetic field. This induced magnetisation varies with the geomagnetic field. The intensity of this induced magnetisation is increased in the thermo-altered zones by the magnetic enhancement produced. As the present geomagnetic field has a direction close to the fossil geomagnetic field for archaeological sites, these permanent and induced magnetisations add up to form a local dipolar magnetic field anomaly, with a magnetic field that is weaker in the north and stronger in the south at the latitude of France. For this reason, hearths or ovens are objects for which geomagnetic prospecting is the preferred method of geophysical imaging.

In prehistoric contexts, there are generally no highly magnetic objects. The geomagnetic anomalies, which reflect the local deformation of the geomagnetic field by these sources, remain moderate in amplitude. In the case of prehistoric caves, surveys are carried out almost in contact with the paleo hearth (Burens et al., 2014; Lévêque and Mathé, 2015; Jaubert et al., 2016). The signal amplitude is then at its maximum. In a coastal situation, the archaeological horizon may be covered by a dune. The thickness of the sand, which increases the distance between the source and the measurement, causes an attenuation of the signal amplitude. This attenuation approximately follows a law inversely proportional to the distance cubed (actually closer to between squared and cubed). In practice, therefore, a moderate source is no longer detectable from a few tens of centimetres to a few metres of vertical distance, depending on its intensity. Source intensity is an unknown a priori. If it is of sufficient intensity to have a detectable signal under the thickness of a dune, then the anomaly will be moderate and spatially extensive. If the source is closer, the intensity of the anomaly will be stronger but have a lower spatial extent.

Apart from the effect of distance from the source, dunes can also produce a topographical effect on the geomagnetic signal. For a terrain with no variation in magnetic properties, the hilltops will be characterised by positive geomagnetic anomalies. Their intensity will be proportional to the magnetic susceptibility of the topsoil horizons because the contrast with the magnetic susceptibility of the air, which is zero, will be all the greater. As a result, the geomagnetic anomaly will be more marked when the relief is higher and the topsoil more magnetic and thicker. In contrast, this effect will be absent for non-magnetic soils, i.e. those with diamagnetic susceptibility for which the iron in the upper horizons is leached out, such as in a podzol.

The vegetation can also be locally thick with bushes. Clearing is sometimes necessary, but this is not always possible for the sake of preserving the biodiversity in protected areas. The distance between the ground surface and the measurement then becomes irregular. To take these effects into account in the analysis of a geomagnetic survey, it is necessary to have a detailed spatialisation of the geomagnetic measurements made and a digital model of the topography in order to determine the distance to the ground for each measurement. Ideally, a spatialisation of the measurements would be performed by laser tracking with a total station (Lévêque and Mathé, 2015). This approach requires the use of a large volume of equipment, which is not always logistically possible to transport, especially on uninhabited islands. In this case, spatialisation can be provided by a GNSS device, but the equipment coupled to the magnetometers have antennas of limited size to minimise magnetic disturbances. Absolute horizontal accuracy does not exceed 0.7 m at best and vertical information is generally not usable.

To cover the area to be surveyed in a homogeneous way, in a topographic context that is generally hilly, visual markers are placed every metre to create parallel lines (fig. 1). The operator walks carrying the measuring device with the help of a frame (fig. 1) allowing them to keep the sensors (at the front of the device) away from sources of magnetic pollution (the acquisition console is in the centre, with the operator, the batteries at the back and the GNSS antenna offset 1.5 m above the sensors). While walking and controlling the recording of measurements on the console, the operator must maintain their alignment with the visual guides.

Finally, the temporal variation of the geomagnetic field, whose amplitude is often similar to that of the signal studied, must be taken into account. The simplest approach, classically used, consists in using gradiometry, i.e. determining the difference in intensity of the total magnetic field (optically pumped magnetometer; fig. 2), called the pseudogradient, or the difference in intensity of the vertical component of the magnetic field (fluxgate gradiometer; fig. 3), called the vertical gradient. Unfortunately, this approach favours sources close to the surface, in the first few decimetres, and the implementation of vertical fluxgate gradiometers requires the sensors to be kept vertical, which is sometimes difficult when the topography is uneven. If the sources are assumed to be further away than the first metre, it is then necessary to work on the intensity of the total geomagnetic field. The temporal variation of the geomagnetic field can then, ideally, be corrected by the variation measured by a second stationary magnetometer located near the surveyed area. This requires having a second magnetometer with identical technology. The alternative is to use the temporal variation of the measurement acquisition, which presents pseudoperiodic variations over the time of a two-way survey trip due to the spatial variations of the magnetic field. The general trend of the temporal variation over the duration of the survey can then be estimated and subtracted from the measurements. This trend will subtract 1) the temporal variation of the geomagnetic field over the duration of a round trip, but also 2) a regional variation of the local magnetic field that is not the object of study. Only short duration variations, of the order of one minute, will not be corrected, but their intensities are generally negligible with respect to the signal studied (less than 1 nT in periods of low geomagnetic activity compared with a signal whose dynamics generally exceed 20 nT, for an average field of 45 000 to 49 000 nT for France).

Fig. 1 – Device of realization of the geomagnetic prospection on the Port Neuf site in Hoedic. The diagonal of coloured field markers planted in the ground corresponds to one of the parallel lines of visual markers placed every meter. The operator follows the alignment of the same coloured field markers, from one line of markers to the next, in order to cover the space evenly. The magnetometer's magnetic field intensity measurement sensors, shown here in the black of the GSMP-35G used, are placed at the front of the carrying structure. The GNSS antenna is offset above the sensors at the end of a pole so as not to pollute the magnetic field intensity measurements. The measurement acquisition console is carried against the operator's midriff. The electronic control units for the sensors and the battery are offset to the rear to limit the pollution from to their movement. This position also allows them to serve as a counterweight (photo P. Arias).

***Fig. 1** – Mise en œuvre de la prospection géomagnétique sur le site de Port Neuf, à Hoedic. La diagonale de fiches de couleur plantées dans le sol correspond aux repères placés tous les mètres, selon des lignes parallèles. L'opérateur suit l'alignement des fiches d'une même couleur, d'une ligne de repère à la suivante, afin de couvrir l'espace de manière homogène. Les capteurs de mesure d'intensité du champ magnétique du magnétomètre (GSMP-35G), ici de couleur noire, sont disposés à l'avant de la structure de portage. L'antenne GNSS est déportée au-dessus des capteurs, à l'extrémité d'une perche pour ne pas polluer les mesures d'intensité de champ magnétique. La console d'acquisition des mesures est plaquée sur le ventre de l'opérateur. Les boîtiers électroniques de contrôle des capteurs et la batterie sont déportés sur l'arrière pour limiter les pollutions liées à leur déplacement ; ils servent aussi de contrepoids (cliché P. Arias).*

1.2. Interpretation of the measurements

Having addressed the issue of measurement recording, we must move on to measurement interpretation. The presence of anomalies following curves or alignments is not necessarily a sure sign of archaeological information. Indeed, both the geological and pedo-geomorphological contexts must be considered. We will take the example of the coastline of the Armorican massif, which is primarily crystalline. Although less magnetic rocks (granites, gneiss and schists) dominate here, other much more magnetic rocks of basaltic composition are also present as veins, due to the Hercynian orogeny. These magnetic veins in much less magnetic rocks lead to linear magnetic anomalies.

The soils that develop on these crystalline massifs, which have high porosity, tend to leach the iron present on the surface causing it to migrate to the interface of the alterite, where it concentrates. This iron accumulation horizon has a high magnetic susceptibility. If erosion brings this deep horizon to the surface, then this outcrop margin will manifest itself as a positive anomaly that follows the topography of the alteration surface.

In order to identify these cases, it is necessary to combine geomagnetic surveys with those using a magnetic susceptibility meter, or kappameter, which is a contact measurement instrument (fig. 4) that determines the capacity of a material to acquire magnetisation when subjected to a magnetic field (weak in this case) in order to determine the variations in magnetic susceptibility of the profiles of the soils and materials present at the outcrop.

2. STUDY OF THE PORT NEUF SITE (HOEDIC ISLAND, MORBIHAN)

2.1. Presentation of the site

The Port Neuf site is a Mesolithic site where burials were made, associated with shell deposits, hearths, lithic material and food bone waste. This site was excavated between 1931 and 1934 by the Péquart couple (Péquart and Péquart, 1954). It is located on the edge of the coast in the north-western part of Hoedic island (fig. 5 and 6), in a dune sector covered by very sparse vegetation, apart from a few bushes (fig. 7).

During the Late Mesolithic, the age of occupation of the Port Neuf site, the Houat and Hoedic archipelago (fig. 5B) was isolated from the mainland by the sub-

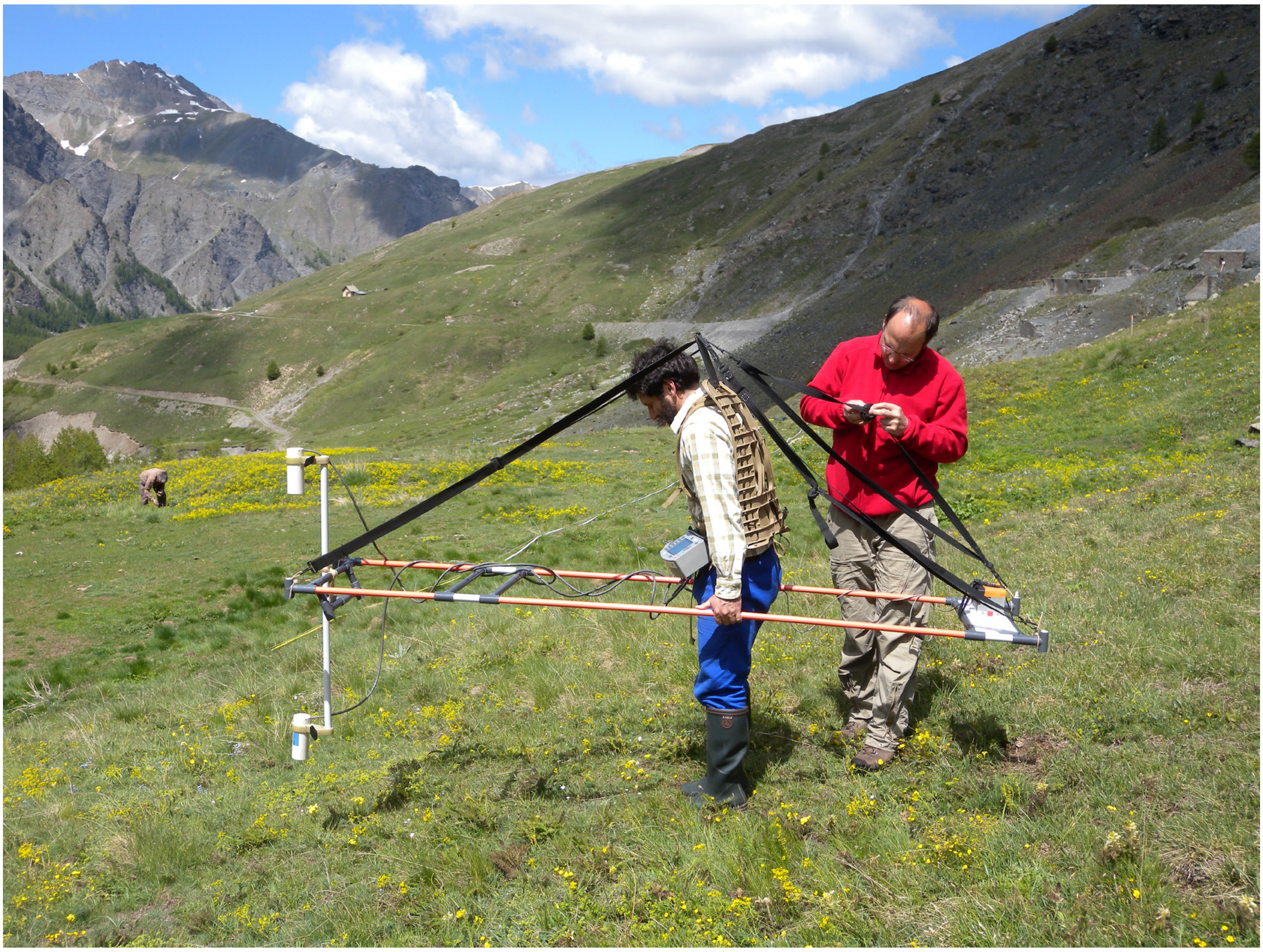

Fig. 2 – Sensor arrangement of a G858 Geometrics optically pumped magnetometer in a gradiometer (photo L. Carozza).
***Fig 2** – Disposition des capteurs d'un magnétomètre à pompage optique G858 Geometrics en gradiomètre (cliché L. Carozza).*

Fig. 3 – Vertical fluxgate gradiometer FEREX (Foerster Holding GmbH) with four sensors mounted on a carrying frame. The operator follows a line marked by a cord (photo V. Mathé).

***Fig. 3** – Gradiomètre vertical fluxgate FEREX (Foerster Holding GmbH) avec quatre capteurs montés sur un châssis de portage. L'opérateur suit la ligne matérialisée par une cordelette (cliché V. Mathé).*

merged Vilaine valley to the north and the Artimon valley to the east (Menier et al., 2006). The break in continuity between these two islands occurred during the Mesolithic. The analysis of recent bathymetric data (fig. 5B), seems to indicate that this break could have occurred before the occupation of the Port Neuf site, contrary to what is generally accepted (Menier et al., 2009). This analysis, based solely on the current bathymetry, remains highly hypothetical as the extent of the erosion of the submerged land surfaces remains unknown. In any case, the site appears to overhang the bay located to the north of the island, a few hundred metres from the shore.

The excavations carried out by the Péquart couple at Hoedic (1931-1934; Péquart and Péquart, 1954), but also on the island of Téviec (1928-1930; Péquart and Péquart, 1929) some twenty kilometres north-east of Hoedic, provided one of the richest funerary assemblages of the last hunter-gatherers in Europe. The human remains and associated archaeological objects have been one of the main sources of information on the Late Mesolithic of western Europe. However, the success of reanalysis of this material with recent isotope or paleogenomic techniques has been limited despite the quality of the Péquart excavation and the good conservation of the collections. The chal-

Fig. 4 – Implementation of susceptibility meters by contact measurement. A: MS2K (Bartington) computer controlled with its MS3 electronics. The advantage of this probe is its small diameter, about 2.5 cm, but the downside is its shallow depth of investigation, of about 1 cm. B: KT9 (Exploranium). The advantage of this instrument is its speed of measurement. The probe diameter of about 6 cm provides a detection depth of 2 to 3 cm. A measurement in air is necessary before and after the measurement carried out in contact with the measured surface.

Fig. 4 *– Mise en œuvre de susceptibilimètres par mesure de contact. A : MS2K (Bartigton) piloté par ordinateur avec son électronique MS3. L'avantage de cette sonde est son faible diamètre, environ 2,5 cm ; le corollaire est sa faible profondeur d'investigation, de l'ordre de 1 cm. B : KT9 (Exploranium). L'avantage de cet instrument est sa rapidité de mesure. Le diamètre de la sonde, environ 6 cm, apporte une profondeur de détection de 2 à 3 cm. Une mesure dans l'air est nécessaire avant et après la mesure réalisée au contact de la surface mesurée.*

lenge is, therefore, to resume the excavation to clarify the chronologies and obtain fresh material. As the site is in a protected area, it is necessary to limit excavations. The use of geophysical imagery is, therefore, necessary both to find the extent of the 1930s excavation and to identify the location/s of potential remains.

2.2. Geophysical surveying problematic

Several geophysical surveys, conducted by several teams using different methods, were carried out on the site with the aim of resuming this excavation. In this article, only results associated with the total field geomagnetic survey and the complementary measurements of apparent magnetic susceptibility are presented. To supplement this mapping information, magnetic susceptibility and viscosity measurements were made using contact sensors on sections after the opening of an archaeological pit.

The presumed presence of hearths in the area not opened in the 1930s is a good reason for using geomagnetic prospecting. The sparse vegetation is favourable to both easy movement and keeping the sensors close to the ground, except for two bushes which would need to be removed for the area to be surveyed. The constraints of the environmental protection of this Natura 2000 site means that this is not possible, however. The presence of a dune complex, one or more metres thick, covering the site is a factor that causes signal attenuation and lateral spreading of the observable anomalies. Indeed, the sand layer separates potential magnetic sources, such as hearths, from the measurements made at the surface, thus reducing the signal. The topography is another tricky aspect that complicates both the implementation of the survey and the interpretation of the signal. Indeed, the surface is marked by decametric undulations, with a vertical amplitude in metres. The most marked slope corresponds to the edge of a mound. In the immediate vicinity of this mound are the remains of a telegraph relay (fig. 7) with a solid metal door, which is a major source of magnetic pollution in the area. In the 1970s this area was also used as a wilderness camping area before the municipal campground was created. The presence of metallic remains (nails, tent pegs, etc.) of this recent occupation on the surface is a concern, as it may be another source of potential magnetic pollution. As the measurements are made in the immediate vicinity of such potential sources, close to the surface, the anomalies they generate will be of high intensity and low spatial extent and, therefore, easily identifiable. In view of all these elements, the chances that a geomagnetic survey could successfully identify hearths appear to be mixed. However, as it is not possible to predict the intensity of the sources associated with the presumed hearths or their depth of burial, only by actually prospecting can we determine its relevance.

2.3. Investigation methods and measuring instruments

The geomagnetic survey presented here was carried out in 'total field', i.e. by measuring the intensity of the magnetic field. This method is preferable to vertical gradiometry when the sources are buried and of moderate intensity. Indeed, gradiometry is efficient in the case of high gradients, for example those associated with (1) highly magnetic sources and/or those located at the surface, such as abandoned explosive devices left over from

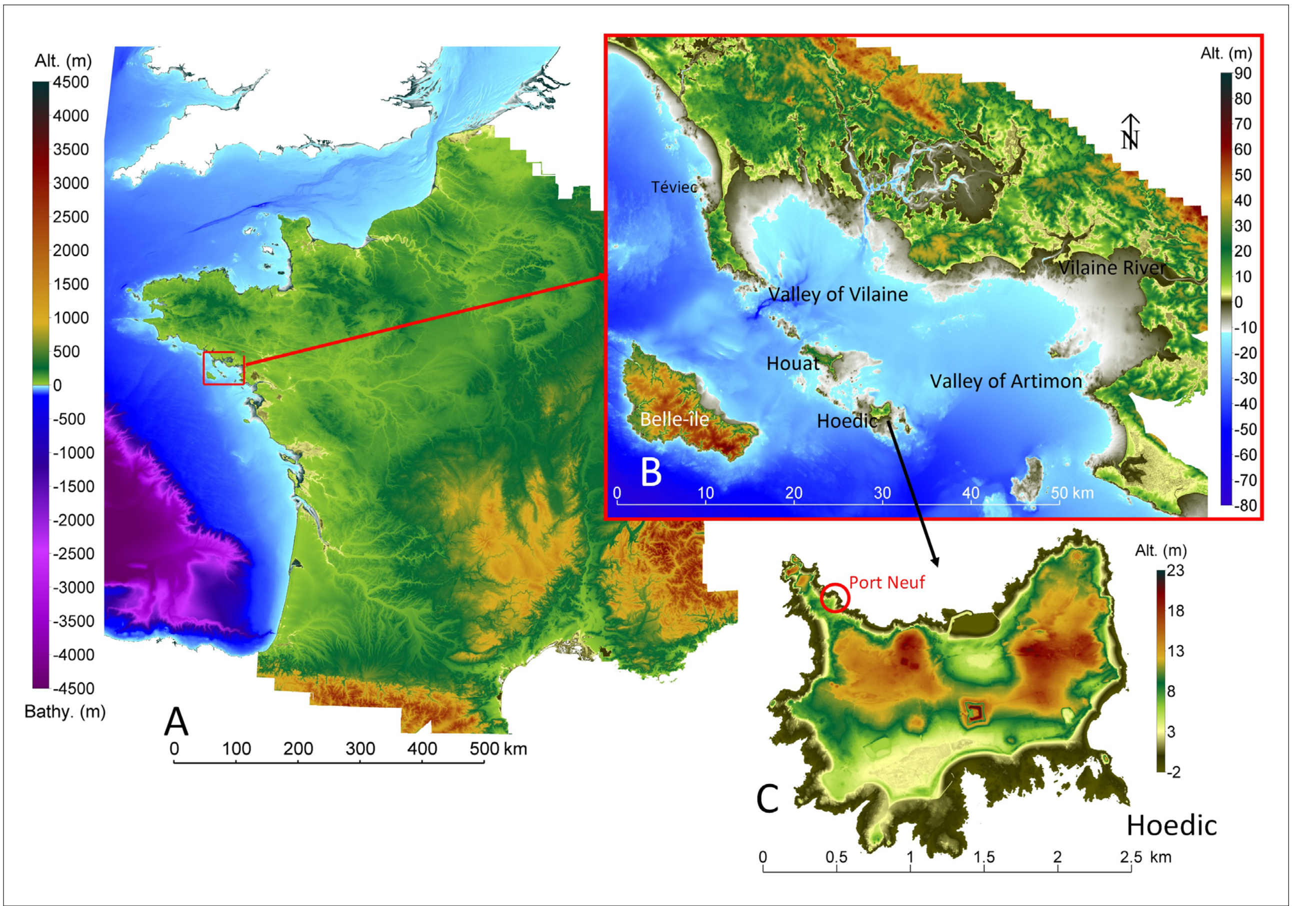

Fig. 5 – Paleogeographic context of the Port Neuf site. The maps were produced in RGF93 Lambert 93 projection. The bathymetric and altimetric levels -12, -11.5, 0 and 3 m are systematically represented in light blue, white, black and yellow, respectively. The levels -12 and -11.5 m, taken arbitrarily, can be considered as a low tide level during the spring tide at a period corresponding to the end of the Mesolithic period (considering a retreat of the order of 3 m at low tide and an isostatic rebound of the order of 1 m since this period, the sea level considered would be of the order of -8 m in relation to the mean reference level). A: Location map of the study area. The map was produced from DTMs from SHOM (2015a), for bathymetry, and from IGN (RGEALTI, 2018) for the altimetry of the map of France. The reference datum is the mean sea level. B: Map of the Morbihan area obtained from the SHOM coastal topo-bathymetric DTM (2015b). C: Topographic map of Hoedic Island obtained from the RGEALTI 1 m DTM (RGEALTI, 2021). The location of the Mesolithic site of Port Neuf is shown by a red circle.

***Fig. 5** – Contexte paléogéographique du site de Port Neuf. Les cartes sont réalisées en projection RGF93 Lambert 93. Les cotes bathymétriques et altimétriques -12 m, -11,5 m, 0 m et 3 m sont systématiquement représentées respectivement par les couleurs bleu clair, blanc, noir et jaune. Les cotes -12 m et -11,5 m, prises arbitrairement, peuvent être considérées comme un niveau de basse mer en vives eaux à une période correspondant à la fin du Mésolithique (en considérant un retrait de l'ordre de 3 m à basse mer et un rebond isostatique de l'ordre de 1 m depuis cette période, le niveau marin considéré serait de l'ordre de -8 m par rapport au niveau moyen de référence). A : carte de localisation de la zone d'étude. La carte est produite à partir des MNT du SHOM (2015a), pour la bathymétrie, et de l'IGN (RGEALTI, 2018), pour l'altimétrie de la carte de la France. Le zéro altimétrique de référence correspond au niveau marin moyen. B : carte du secteur du Morbihan obtenue à partir du MNT topo-bathymétrique côtier du SHOM (2015b). C : Carte topographique de l'île de Hoedic réalisée à partir du MNT RGEALTI 1m (RGEALTI, 2021). La localisation du site mésolithique de Port Neuf est figurée par un cercle rouge.*

the wars of the 20th century, or (2) material contrasts over large volumes, such as the edges of ditch fillings done with magnetic soils in a surrounding material that is not very magnetic.

The magnetometer used was an optically pumped magnetometer GSMP-35G (GEM System; fig. 1), which offers the advantage of being able to measure the intensity of the magnetic field at a rate of 20 measurements per second, with an instrumental sensitivity of 0.0015 nT at this frequency, i.e. well above one millionth of the earth's field. This sensitivity is much finer than the effective repeatability of the measurements, which can be estimated at a value between 0.1 and 0.5 nT according to the configuration of the device implementing the magnetometer. Indeed, the presence of the battery, which is discharging current, and the measuring console, whose position in relation to the sensors and the direction of the magnetic field is constantly changing, generate disturbances. To minimize this effect, a homemade carrying frame has been designed to move the sensors to the front and the batteries to the rear, thus acting as a counterweight. The console is attached to the operator to ensure that it wobbles as little as possible and allows them to follow the recording of the measurements (fig. 1). Ideally, this console could also be positioned as a counterweight to move it away from the sensors, but then the operator would no longer be able to verify the correct recording of the measurements so this set-up was not chosen for the present study.

The profiles, marked on the ground with visual markers spaced 1 m apart, are arranged perpendicularly to the direction of the magnetic field in order to minimize the artifacts generated by the console and batteries. Indeed, if the sensors were aligned in the direction of the mag-

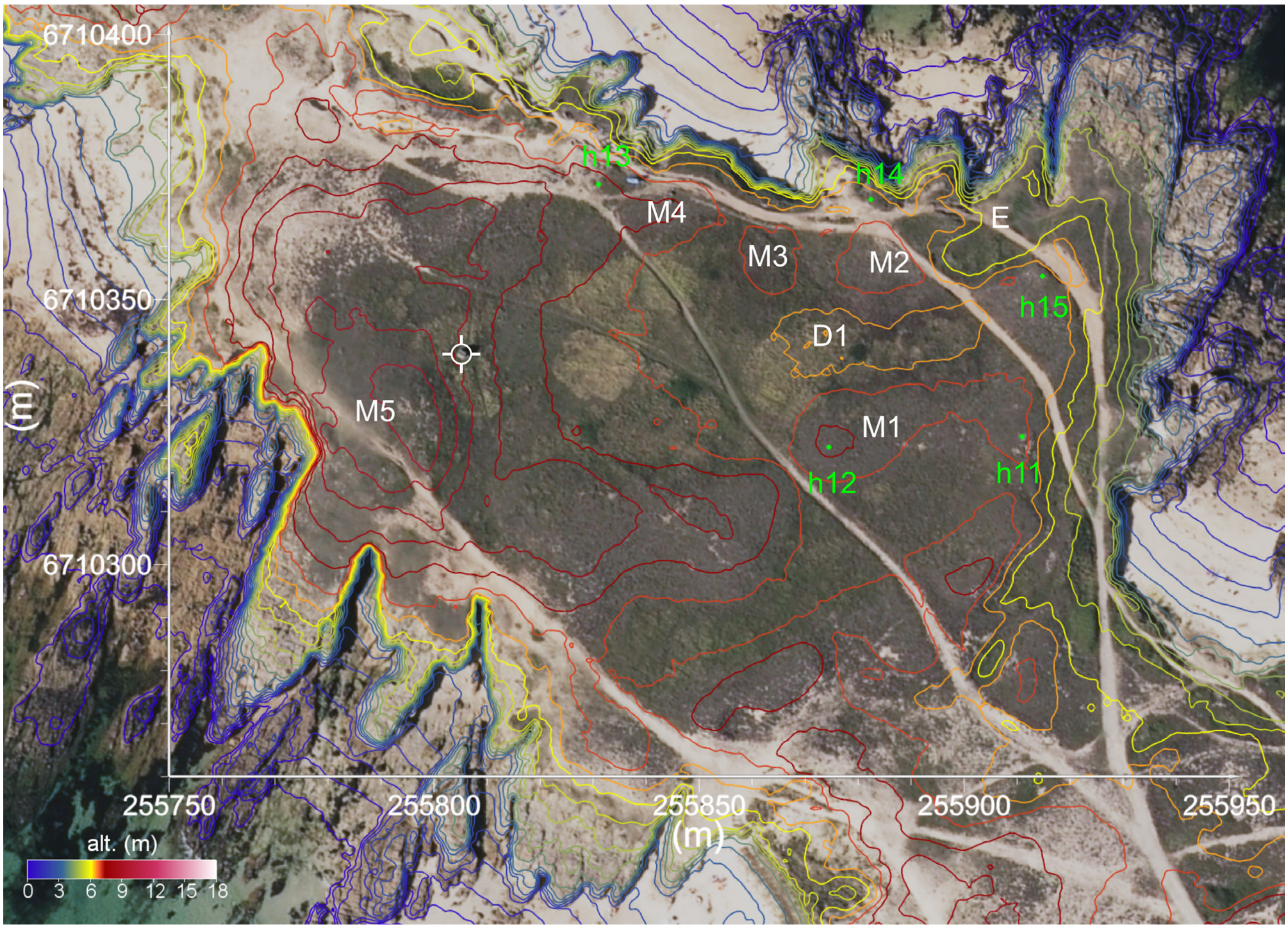

Fig. 6 – Location of the area covered by the geophysical survey on the NW tip of Hoedic island at Port Neuf. The reference used is Lambert93. The orthophotograph is an extract of ORTHOHR_1-0_JP2-E080_LAMB93_D56-2019 (IGN). The contour lines were established from the RGEALTI_FXX_0255_6711_MNT_LAMB93_IGN69 (IGN) and are spaced at 0.5-m intervals. E: area of the 1930s excavation (Péquart and Péquart, 1954). M1 to M5: topographical mounds; D1: topographical depression; h11 to h15: spatial reference marked by green dots corresponding to metal rods driven vertically into the ground. The remains of the telegraph relay station are indicated by the symbol ⌖.

Fig. 6 *– Localisation du secteur couvert par la prospection géophysique sur la pointe NW de l'île d'Hoedic à Port neuf. Le référentiel utilisé est Lambert93. L'orthophotographie correspond à un extrait de ORTHOHR_1-0_JP2-E080_LAMB93_D56-2019 (IGN). Les courbes de niveaux sont espacées de 0,5 m. Elles ont été établies à partir du RGEALTI_FXX_0255_6711_MNT_LAMB93_IGN69 (IGN). E : secteur de la fouille des années 1930 (Péquart et Péquart, 1954). M1 à M5 : buttes topographiques ; D1 : dépression topographique ; h11 à h15 : référence spatiale matérialisée par des points verts correspondant à des tiges métalliques enfoncées verticalement dans le sol. Les vestiges du poste de relais télégraphique sont marqués par le symbole ⌖.*

Fig. 7 – View of the vegetation cover of the Port Neuf site. A first line of field markers is visible in the foreground and a second one can be seen about 30 m away. The building visibly standing out on the skyline is the remains of the telegraph relay station.
Fig. 7 *– Vue du couvert végétal du site de Port Neuf. Une première ligne de repère est visible au premier plan ; une seconde se distingue à une trentaine de mètre. La construction visible se détachant sur la ligne d'horizon correspond aux vestiges du relais télégraphique.*

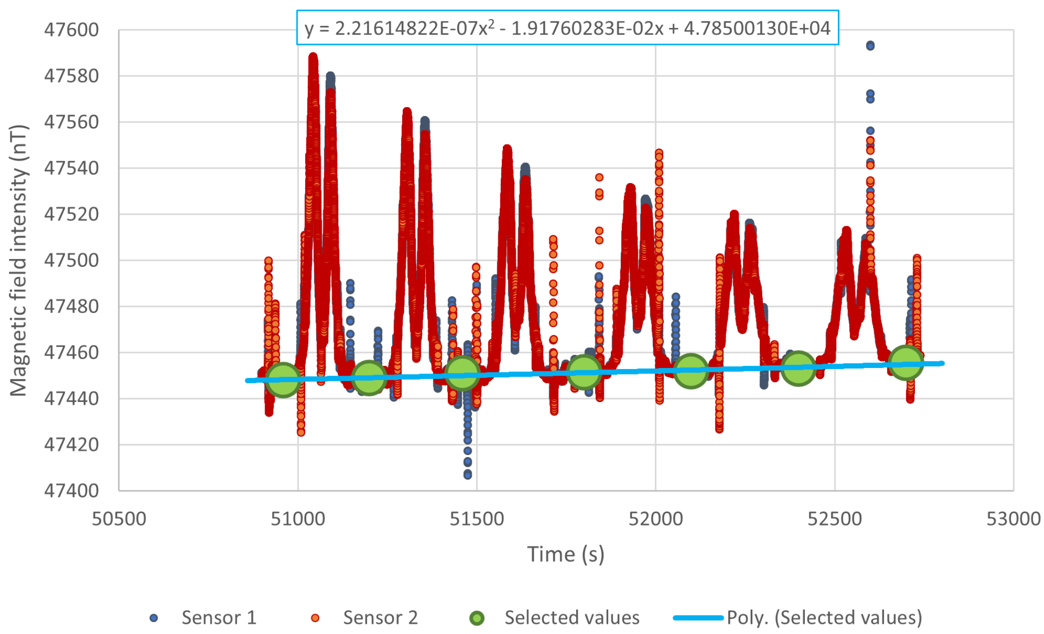

Fig. 8 – Correction of the variation of the magnetic field with time. A polynomial function, used as an estimator of the temporal variation of the magnetic field strength, is determined by fitting selected values considered as median with respect to the observed variation. The round trips generate a pseudoperiodic structure whose extreme values correspond to passage close to magnetic sources. These temporal variations linked to the displacement are not taken into account when bulding the polynomial function equation.
Fig. 8 *– Correction de la variation temporelle du champ magnétique. Une fonction polynomiale, utilisée en tant qu'estimateur de la variation temporelle de l'intensité du champ magnétique, est déterminée par ajustement de valeurs sélectionnées considérées comme médianes par rapport à la variation constatée. Les allers-retours génèrent une structure pseudopériodique dont les valeurs extrêmes correspondent au passage à proximité de sources magnétiques. Ces variations temporelles liées au déplacement ne sont pas prises en compte pour la recherche de l'équation de la fonction polynomiale.*

netic field with these sources of magnetic disturbance, then their influence would be at its maximum. The two sensors are spaced 0.5 m apart horizontally and held by the operator at about 0.2 m above the ground. At a speed of movement of the order of 1 m/s, each round trip makes it possible to acquire two lines of measurements with 20 measurements per metre for each trip, i.e. 40 measurements per metre. The homogeneity of the distribution of measurement points along the ground depends on the evenness of the operator's movement. The temporal variation of the magnetic field is corrected by the removal of a polynomial function passing through the median values of the measured temporal variation exploiting the pseudoperiodic variation of the round trips as mentioned at the end of section 2.1 (fig. 8).

This magnetometer has a GNSS satellite positioning system of the SBAS type with an absolute horizonal accuracy of 0.7 m. For successive measurements over a short time, the relative accuracy is better. The vertical position is recorded with an accuracy in metres. This accuracy is insufficient to obtain relevant height information in the dynamic topographic setting of the Port Neuf site. It would have been preferable to double the positioning of the measurements by laser tracking of a reflector fixed on the carrying structure, using a motorised total station (Lévêque and Mathé, 2015). This approach would allow a positioning accuracy of the order of a few centimetres in all directions in space (the main error comes from the reflector not remaining vertical with respect to the sensors on slopes). The choice was made not to use a total station here, mostly because of the need to reduce the volume of material to be transported, a choice that proved to be detrimental.

The apparent magnetic susceptibility measurements were carried out with a GEM 2 conductivity meter (Geophex, Ltd.; fig. 9). Just as in geomagnetic prospecting, measurement with a conductivity meter does not involve contact with the ground. However, this method, known as electromagnetic, is an active method, unlike geomagnetic prospecting, which is a passive method. A transmitter coil generates a magnetic wave that propagates in the ground. Depending on the electrical and magnetic properties of the surroundings, the magnetic field produced will generate induced electric currents and induced magnetisations, respectively. The latter will, in turn, generate a secondary magnetic field, the variations of which are measured by a

Fig. 9 – Implementation of the GEM 2 conductivity meter (Geophex, Ltd). The GNSS antenna is placed at the end of a mast to maintain a constant relative position between the measurement and the determination of its position. The carrying device, made of neutral materials (plastic and fibreglass tube), helps to keep the conductivity meter horizontal as the operator is walking (photo P. Arias).

***Fig. 9** – Mise en œuvre du conductivimètre GEM 2 (Geophex, Ltd). L'antenne GNSS est disposée à l'extrémité d'un mat permettant de conserver une position relative constante entre la mesure et la détermination de son positionnement. Le dispositif de portage, réalisé en matériaux neutres (plastique et tube en fibre de verre), favorise le maintien de l'horizontalité du conductivimètre tout en marchant (cliché P. Arias).*

receiver coil, distant from the first (transmitter) coil. The original signal will be distorted according to the capacity of the environment to conduct the magnetic field and the electric current. These two properties correspond to two physical quantities, the magnetic susceptibility (which is magnetic permeability expressed in another form) and the electrical conductivity.

The distance between the transmitting and receiving coils is approximately 1.6 m. The depth of investigation and the volume of the ground explored depend on the electrical properties of this environment and the height of the instrument above the ground. Surveying is carried out trying to keep the device horizontal at about 0.3 m above the surface (the minimum distance needed to minimise correction artefacts from the instrumental drift compensation coil, situated between the transmitting and receiving coils). Although it is difficult to estimate this depth of investigation, we can consider that it is of the order of the spacing between the coils, from must be subtracted the height of surveying, i.e. approximately 1.3 m (value of the probable response, knowing that part of the signal potentially reaches down to 10-20 m depth). The volume of investigation is then calculated in m^3.

Magnetic susceptibility measurements were carried out using contact sensors (fig. 4). The KT9 (Exploranium) is used for fast measurements on areas of about 6 cm in diameter. With this type of sensor, the signal produced by a magnetic source decreases with the distance between the sensor surface and the object of interest. For a homogeneous material, 95% of the signal comes from a detection volume of about 150 cm^3 for a penetration depth of 3 cm (Lecoanet et al., 1999). For higher spatial resolution profiles, the MS3 control unit (Bartington) and the probe MS2K, with a detection diameter of about 2.5 cm, were used. These measurements were complemented by magnetic viscosity measurements made with the similar 2.5 cm diameter MVM1 probe (Pulsepower Developments; fig. 10). The reduction in sensor diameter results in a reduction in detection volume and depth of investigation, which does not exceed 1 cm for the MS2K probe.

2.4. Geomagnetic mapping

The geomagnetic mapping of the Port Neuf area is shown in figure 11. The metal door of the telegraph relay generates a major dipole anomaly (negative pole in blue to the north, positive pole in red to the south), impacting the western half of the covered area. Smaller dipoles appear in a line northward of the telegraph relay (only the positive parts stand out). One remedy for these strong spatial variations is to observe only the variations on a sub-metric scale. To do this, it is sufficient to calculate the local horizontal gradient by the difference between the two sensors (fig. 12). This approach also has the advantage of eliminating temporal variation while attenuating major large-scale anomalies. Sub-metric anomalies, from point sources close to the surface, are thus well isolated. This information is similar to what would be produced by a vertical gradient survey. However, anomalies greater than a metre in size and from a much deeper source disappear because the signal they produce at the surface is very similar viewed from the positions of each of the two sensors.

To try to distinguish the minor anomalies present in the western area under the influence of the telegraph relay anomaly, another solution consists in subtracting the general trend from the main dipole structure. The magnetic anomaly generated by the main source is simulated by a simple mathematical model approximating the structure of a real magnetic anomaly:

$$\left(\frac{Y}{\sqrt{Y^2}}\right)\cdot\left(\frac{(\alpha.X)^2}{((\alpha.X)^2+(\beta.Y)^2)^3}\right)^{\gamma}$$

α, β and γ are fit variables of the model and X and Y are the horizontal coordinates. A translation and rotation of X and Y is performed to centre and orient the mathematical model generated. The version presented in figure 13 has been empirically optimised. Although a model closer to the main variation can certainly be obtained, it is not necessary to improve the fit. Indeed, once subtracted from the data, it appears (fig. 14) that the edges of the anomaly in the sloping areas near the telegraph relay show shifts between two successive profiles. This shift is due to differences in the altitude of the sensors between the profiles made during ascent and descent because the distance to the source is different. Furthermore, there is also a shift in horizontal positioning caused by the failure to maintain verticality between the GPS antenna and the sensors. It should, therefore, be possible to correct the effects of this horizontal shift and, above all, to take into account the differences in altitude in the model so as to significantly improve it. Unfortunately, there is too little precision in the determination of the altitude to obtain a reasonable correction of these effects with the set-up used here.

The analysis of the anomalies extracted after correction of the major anomaly (fig. 14) shows two linear structures starting almost at right angles to the telegraph relay. These anomalies correspond to the cables linking with the mainland to the NNE and the centre of the island to the ESE, which are visible on the ground locally. In addition, several dipolar anomalies stand out to the north of the relay. Considering the intensities, these correspond to metallic masses, either related to the telegraph relay or to a historical use of the sector as a rubbish dump (P. Buttin, Pers. Comm.).

A series of isolated anomalies, ranging in size from metric to sub-metric, are clearly identified (red ellipses; fig. 14). These anomalies were already identifiable on the horizontal gradient representation (fig. 12), but less marked than those observable with the corrected total field (fig. 14). They are sometimes aligned in a circle or an arc and seem to be associated with the presence of stone blocks on the surface. A systematic survey would be necessary to clarify this. Indeed, it is unlikely that a stone block of the substrate could produce such geomagnetic anomalies as the material is naturally not very magnetic. Some of these blocks show

Fig. 10 – Recording of magnetic viscosity measurements with an MVM1 (Pulsepower Developments). The measurements are complementary to those made with the KT9 (Exploranium). Magnetic viscosity is an estimator of the concentration of nanometric magnetic phases (ferromagnetic in the broad sense, mainly ferrimagnetic), and is therefore independent of the low or non-magnetic matrix (paramagnetic or diamagnetic), unlike the measurement of magnetic susceptibility. The latter will be sensitive to the enhancement of the magnetic phase, mainly ferrimagnetic. These measurements were successively carried out on the same area (photo P. Arias).

***Fig. 10** – Mise en œuvre de mesures de viscosité magnétique avec un MVM1 (Pulsepower Developments). Les mesures sont complémentaires de celles réalisées avec le KT9 (Exploranium). La viscosité magnétique est un estimateur de la concentration en phases magnétiques (ferromagnétique au sens large, principalement ferrimagnétique) nanométrique, elle est donc indépendante de la matrice peu ou non magnétique (paramagnétique ou diamagnétique), contrairement à la mesure de la susceptibilité magnétique. Cette dernière sera sensible à l'enrichissement en phase magnétique, principalement ferrimagnétique. Ces mesures sont réalisées successivement sur une même surface (cliché P. Arias).*

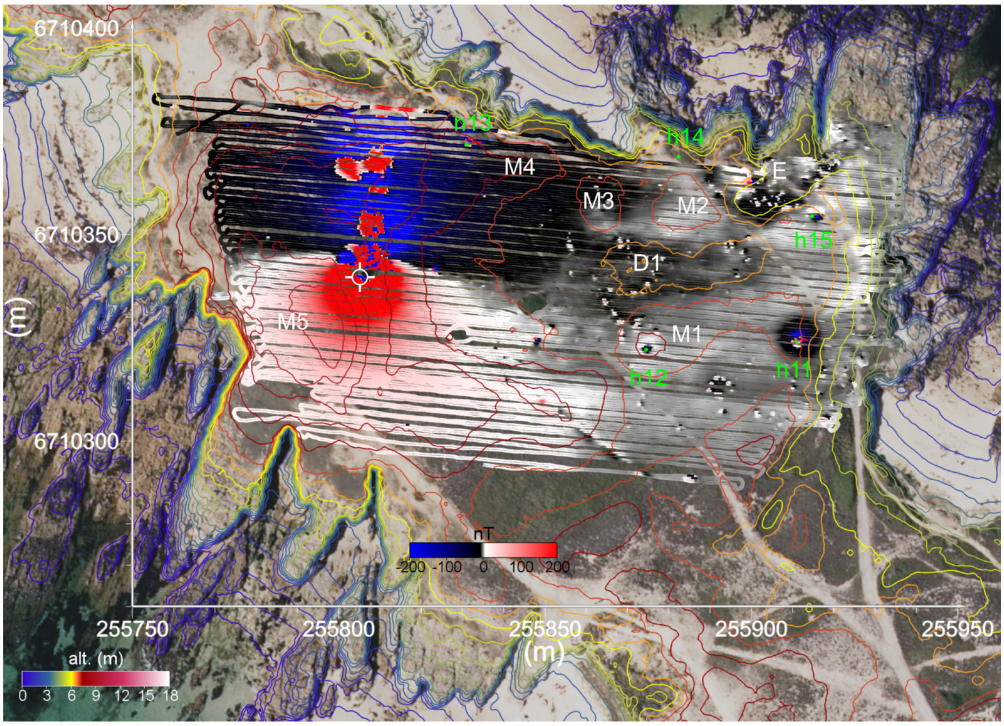

Fig. 11 – Geomagnetic survey of the Port Neuf sector (see legend fig. 1). Each magnetic field intensity measurement is represented by a point whose succession forms the lines along the profiles. The spatial marker h11 is at the centre of the strong anomaly produced by the metal rod. The other four markers are associated with smaller anomalies or are at the edge of the covered area, to the North. (For additional information see the legend fig. 6.)

Fig. 11 *– Prospection géomagnétique du secteur de Port Neuf (voir légende de la figure 1). Chaque mesure d'intensité du champ magnétique est représentée par un point dont la succession forme les lignes selon les profils. Le repère spatial h11 est au centre de la forte anomalie produite par la tige métallique. Les quatre autres repères sont associés à des anomalies plus modestes ou sont en bord de zone couverte, au nord. (Informations complémentaires dans la légende de la figure 6.)*

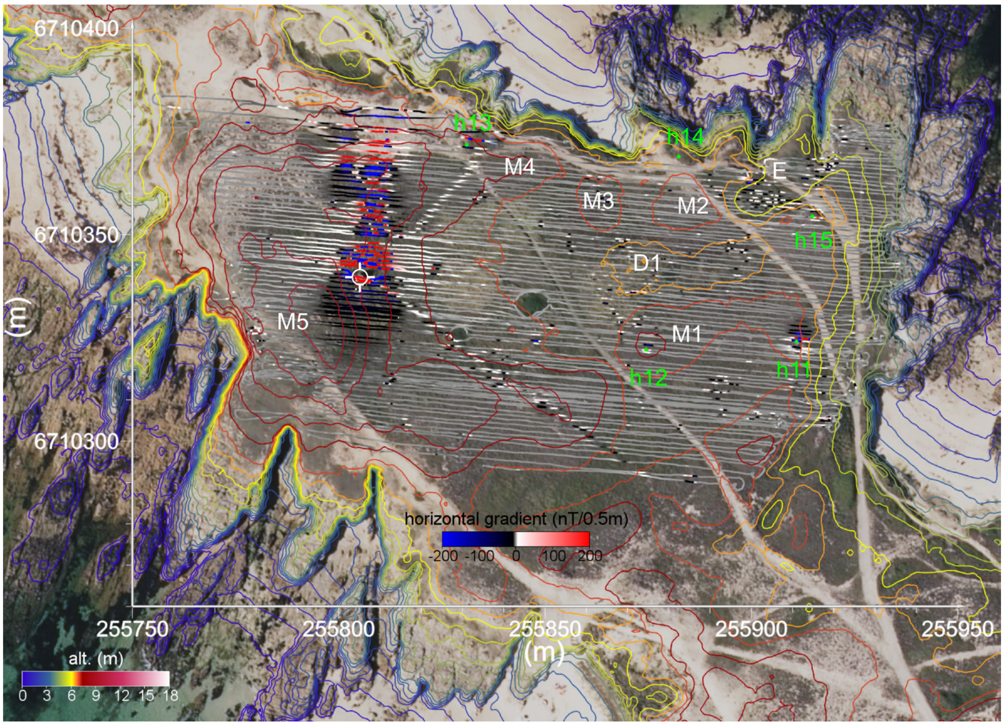

Fig. 12 – Horizontal gradient of the Port Neuf area (see legend fig. 1).
The colour scale is the same, to allow easy comparison. The unit is nT/0.5m rather than nT/m.

Fig. 12 *– Gradient horizontal du secteur de Port Neuf (voir légende figure 1).*
L'échelle de couleur est inchangée pour permettre une comparaison immédiate. Pour cela l'unité est en nT/0,5 m au lieu de nT/m.

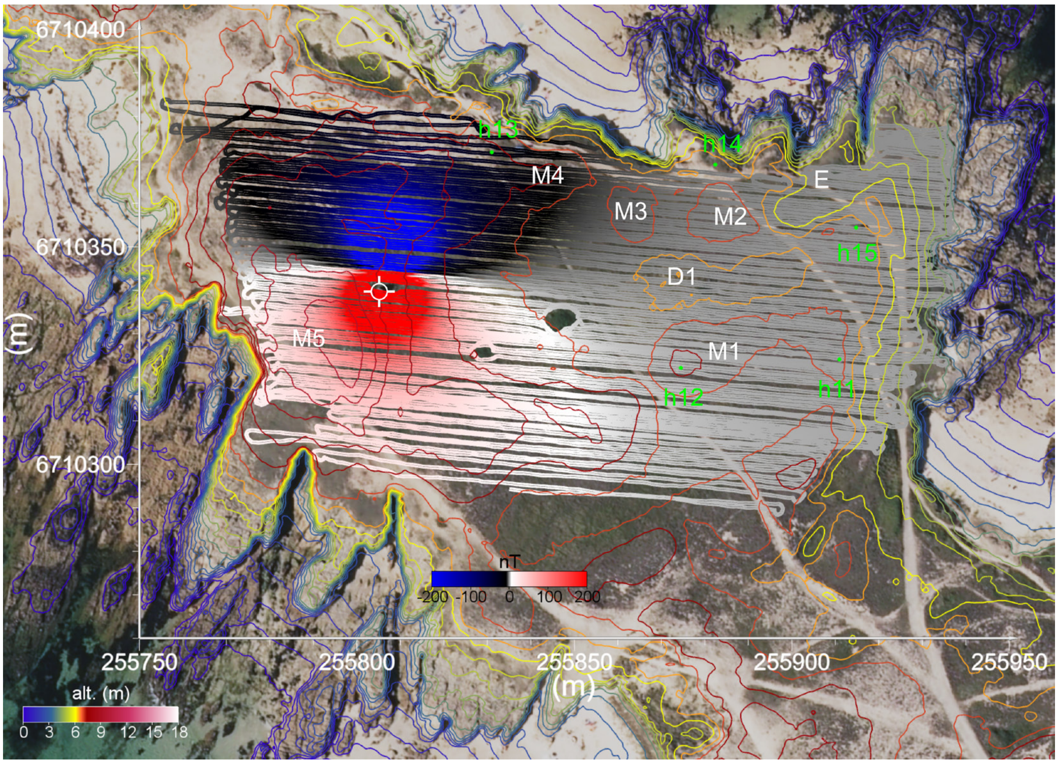

Fig. 13 – Model of the dipole anomaly produced by the remains of the telegraph relay (see legend fig. 6).
Fig. 13 – *Modèle de l'anomalie dipolaire produite par les vestiges du relais télégraphique (voir légende figure 6).*

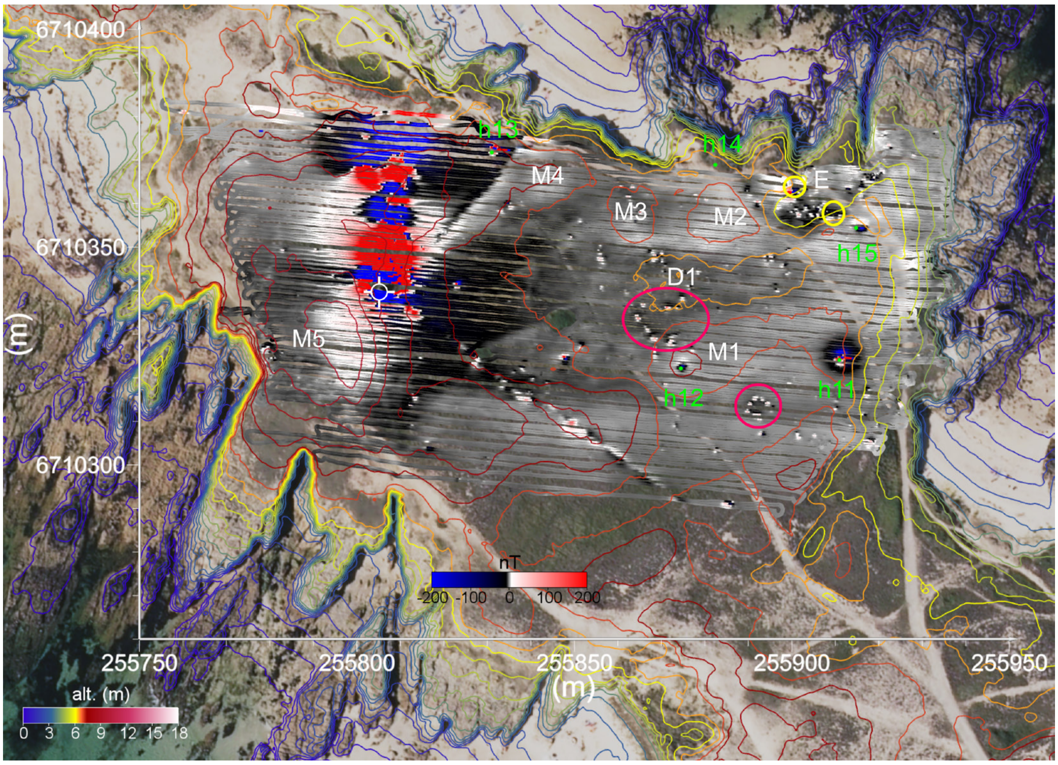

Fig. 14 – Model-corrected total field strength of the major anomaly produced by the telegraph relay door (see legend fig. 6). The red ellipses mark groups of anomalies. The yellow circles in the area of the excavations (E) mark dipolar magnetic sources; the one closest to the h15 mark could be a hearth and the second one a metallic mass due to the E–W orientation of the dipole.
Fig. 14 – *Champ total corrigé du modèle de l'anomalie majeure produite par la porte du relais télégraphique (voir légende figure 6). Les ellipses rouges marquent des groupes d'anomalies. Les cercles jaunes dans la zone des fouilles (E) marquent des sources magnétiques dipolaires qui pourraient correspondre à un foyer, pour la plus proche du repère h15, ou une masse métallique du fait de l'orientation E-W du dipôle, pour la seconde.*

rubefaction of their surfaces. The spatial resolution of the geomagnetic survey, with profiles about 0.5 m apart, does not allow us to say whether these anomalies are dipolar. However, the action of fire on the stone blocks seems likely to have produced the thermo-alterations, as indicated by the rubefaction, but also to have led to the acquisition of strong thermoremanent magnetisations.

The analysis of the data in terms of magnetic field intensity (fig. 14) integrates the correction of the relay effect and thus allows the exploitable area to be extended compared with the gradiometry (fig. 12). Its major interest is to reveal anomalies of weaker intensity and decametric dimensions not visible by gradiometry, such as those to the south of mounds M2, M3 and M4 (fig. 14). The relationship of these decametric anomalies with topographic variations appears complex. The topography here is potentially influenced by the presence of excavated material from the old 1930s excavation (probably the case for the slight relief present to the west of marker E, figure 14, associated with a positive anomaly in its eastern part). Material from deep archaeological horizons, potentially more magnetic, may have been brought to the surface. In this case, the spoil creates a local positive anomaly. In contrast, a similar anomaly may be produced by a deeper, more magnetic source, such as a hearth. The anomalies associated with mounds M2 and M3 and possibly M4 (fig. 14), north of the main depression (D1), could indicate the presence of such objects. To attempt to clarify this interpretation, we conducted an electromagnetic survey.

2.5. Electromagnetic survey

The area covered by the electromagnetic survey was limited to the eastern part of the site (fig. 15 and 16) close to the area of the 1930s excavation with potentially interesting geomagnetic anomalies. The measurements were carried out using a prototype carried device currently under development (a more advanced version of which is illustrated figure 9). Measurements were acquired every 0.12 s with three excitation frequencies, 475, 1575 and 45075 Hz. The swaying of the device relative to the control tablet caused disturbances in the form of high frequency fluctuations in the signal. To mitigate this noise, sliding window smoothing was applied with the median calculated over a 0.84 s window. Only the most representative data with the least noise are presented.

Electric conductivity

The electrical conductivity, proxied by the quadrature signal at 45075 Hz, is shown in figure 15. Its values, marked in blue on the figure, are low, consistent with the southern mound M1 (fig. 15). This mound corresponds to a dry, slightly clayey material. Given the context, this feature must correspond to a dune structure. A similar zone of low conductivity, shown by the yellow and orange contour line, to the north-east, corresponds to the area excavated in the 1930s (E, fig. 15) and extends eastwards. This area appears to be dominated by a very close or outcropping bedrock signal or by the presence of the heap of excavated material to the east. The north-eastern end shows a highly conductive zone which, given its proximity to the sea, must correspond to a zone salted by evaporation of sea spray. A zone of high conductivity lies between the two zones of low conductivity, located between the main depression D1 and the mound M2 (fig. 15). This zone seems to be too far from the area exposed to sea spray that the high conductivity could be explained by a salty environment. Therefore, these high values most certainly indicate a more clayey material. Such clayey layers can be observed on the top of the beach cliff located to the east. They correspond to a layer of alterite, autochthonous or reworked with aeolian deposits, covering the bedrock. This alterite seems to have been preserved from erosion in the depressions of the bedrock. The erosion must have been pre-Mesolithic. Indeed, according to the illustrations of Péquart's observations, the Mesolithic occupations seem to be on this clay layer (Péquart and Péquart, 1954).

The two small elevations, mounds M2 and M3 (fig. 15), to the north of depression D1, have different electrical conductivity. The westernmost of these, M3, has an average conductivity, while the second, M2, shows an offset from the contour lines. We need to ask if this is the result of the accumulation of excavated material from the 1930s, consisting of dune material (low electrical conductivity) to the east and deeper material to the west (higher electrical conductivity due to increased clay content). An analysis of the sediments in the column would be needed to answer this question. To the east of the survey area, the concordance of the two high conductivity anomalies with the position of the paths casts doubt on the origin of the signal. It could be explained by the filling of the roads with materials more clayey than the dune materials. An extension of the survey to the east would be necessary to propose a reliable interpretation.

Apparent magnetic susceptibility

The apparent magnetic susceptibility, proxied by the signal in phase at 1575 Hz (fig. 16), has a very different spatial signature from that of the electrical conductivity. The lowest values recorded in the south-east and at the north-east show very strongly negative values with low consistency indicating that the phase signal values cannot be converted into a true magnetic susceptibility value. Only the relative variations are to be taken into consideration. The high values define a structure located halfway up the slope between the main depression (D1, fig. 16) and the mounds to the north (M2 and M3, fig. 16). The position of this structure, which has a high magnetisation capacity, is south of the positive geomagnetic anomalies associated with the mounds (M2 and M3). There is, therefore, no direct relationship between these geomagnetic anomalies and increases in the magnetising capacity of the materials. There are two possible explanations for this: either the sources of the geomagnetic anomalies are too small with respect to the volume explored for apparent magnetic susceptibility, or their source corresponds

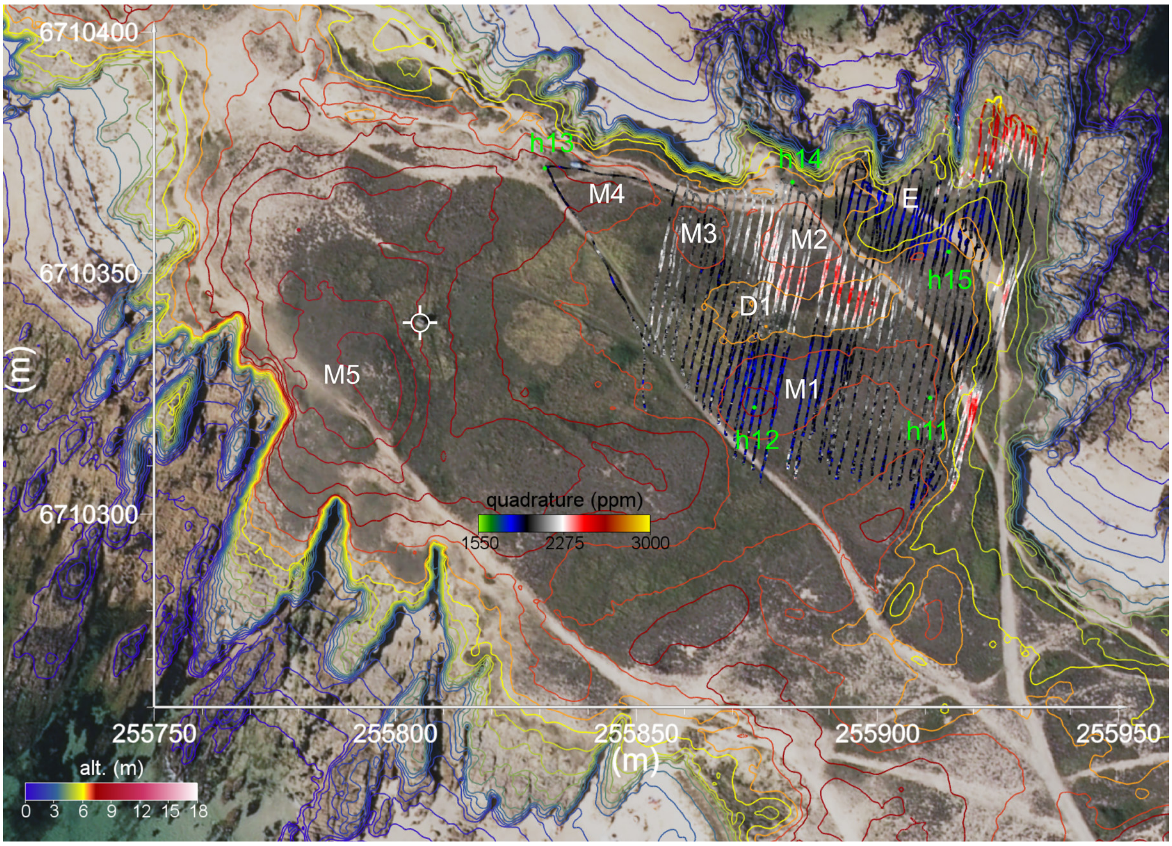

Fig. 15 – Electrical conductivity estimated by the quadrature signal (see legend fig. 6).
***Fig. 15** – Conductivité électrique estimée par le signal en quadrature (voir légende figure 6).*

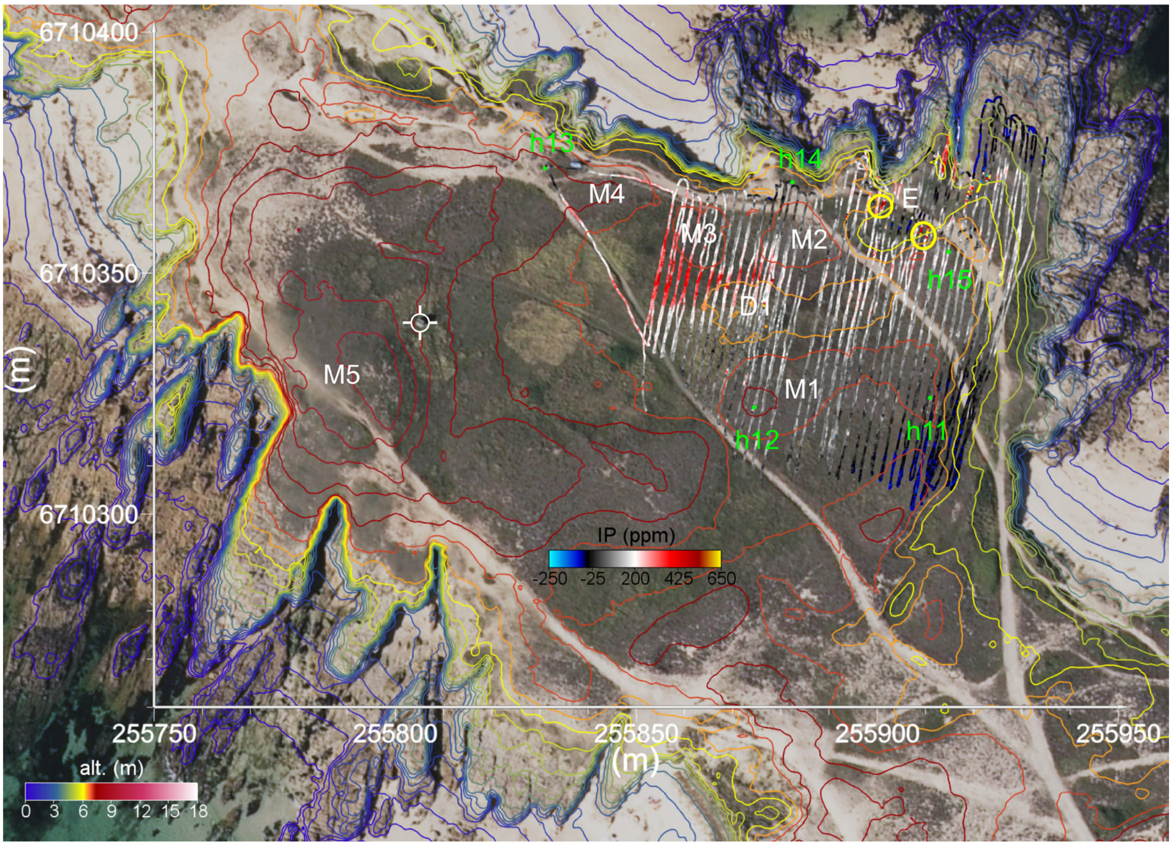

Fig. 16 – Apparent magnetic susceptibility estimated by the phase signal (see legend fig. 6).
***Fig. 16** – Susceptibilité magnétique apparente estimée par le signal en phase (voir légende figure 6).*

mainly to remanent magnetisations such as thermoremanent magnetisations produced by fire. Such magnetisations are not picked up by instruments taking magnetic susceptibility measurements (conductivity meter, susceptibility meter). Only the thermo-alteration effect would be detectable in this case, but the volume involved would be too negligible to generate a significant signal. However, this structure of high apparent magnetic susceptibility reflects the presence of more magnetic materials than the poorly magnetic dune environment. The layer of alterite already mentioned may be locally close to the surface. It certainly has a higher magnetic susceptibility than the levels of the dune. Its magnetic susceptibility may also have been locally increased by the action of pedogenesis or by human occupation, which would have produced magnetic enhancement.

The excavation area (E, fig. 16) is complex. In the north, the high values are related to the remains of a motor embedded in a fault between the rocks. Overall, the excavated area has low values, which reflect the outcropping of the bedrock. This is because the bedrock has a low magnetic susceptibility. At the southern edge of this depression, positive values define an anomaly of more than 2 m at the limit of the yellow contour line (yellow ellipse, fig. 16). This apparent positive magnetic susceptibility anomaly is at the limit of the slope break and the survey profiles are sub-perpendicular to it. This 'step' is the source of an artefact caused by the failure to maintain the conductivity meter horizontal and at a constant distance from the ground. However, the consistency of the two successive profiles, first in one direction and then the return, supports the presence of a magnetic source. The electrical conductivity shows no variation in this sector, indicating no metallic mass, but does not indicate any anomaly around the motor remains either. However, a geomagnetic dipole anomaly coincides with these high apparent magnetic susceptibility values. This geomagnetic anomaly could, therefore, indicate the presence of a hearth. However, a slight spatial offset cannot be ruled out, but remains within the relative inaccuracy of the satellite positioning of the two instruments. These findings, therefore, support the probable presence of a hearth at the edge of the area stripped in the 1930s.

A second individual analogous positive anomaly is located about 10 m to the NW (yellow circle, fig. 16). However, in this case, it is associated with a very strong geomagnetic dipole anomaly whose dipole axis is very far from magnetic north, suggesting the presence of a ferrous metal artefact, such as that which was identified in the 2021 test pit.

3. SUMMARY AND SYNTHESIS

When there is dune surface cover, as in the case of the Port Neuf site, an archaeological hearth seems to produce a moderate geomagnetic anomaly. The attenuation of this anomaly is, therefore, rapid with distance. Its identification is only robust in places where the covering of the hearths is thin, such as in the area excavated in the 1930s (yellow circle close to h15, fig. 14). The anomalies associated with mounds M2 and M3 (fig. 14) are still potential hearth targets but are much more uncertain. Indeed, these anomalies are well associated with variations in apparent magnetic susceptibility, but their positions are shifted. The origin of the geomagnetic anomalies in mounds M2 and M3 could also be the result of a topographic effect associated with a more magnetic fill. To propose a reliable interpretation of the observations, it would be necessary to carry out core sampling or sondage to study the variations in the magnetic properties of the sedimentary column in this area.

Apart from the anomalies associated with the telegraph relay, the isolated anomalies associated with the boulders could be related to recent activity. However, the position of the excavation area observed on the aerial photograph from 1932 does not seem to correspond (red ellipse between E and M2, fig. 17). The Péquart camp is located at the western end of the central depression D1 (red ellipse, fig. 17), while the nearest anomalies are spread along the northern and southern edges of this depression. This aerial view allows us to propose a reconstruction of the position of the past excavation of the four successive years according to the superposition of the diagram published in 1954 (Péquart and Péquart, 1954). The geomagnetic anomalies associated with the SW and SE sides of the excavated area could be associated with the edges of the dig. In this case, an offset of 1.5 m to the east and south would be required to match these edges with the anomalies.

In the vicinity of this excavation area, measurements were made using contact sensors to observe the variations in magnetic susceptibility in situ. The variations observed on three vertical profiles of the same trench, about 0.5 m apart, show strong similarities overall (fig. 18). The two extreme profiles allow the identification of variations associated with the melanisation of certain horizons. These organic levels are associated with low magnetic susceptibility values, as is the surface horizon. These black horizons, therefore, appear to be palaeosols, the horizon of organic accumulation that led to the leaching of iron. Their formation would correspond to three periods without aeolian inputs –including the present one – or at least to a marked slowing down of these inputs. If we can draw a parallel with the loess of China (Maher, 2011), these periods of increased pedogenesis would potentially correspond to warmer and wetter periods. It should be noted, however, that the loess cycles in China are on a different time scale. They are produced by the forcing of the Earth's orbital cycles, specifically the cycles of precession of the equinoxes, with a period of around 20 ky. Similarly, the pedogenesis of loess, which is more clayey than dune materials, generates a magnetic enhancement of the soil, whereas layers of soil on dune sands cause a depletion of the magnetic phase through iron leaching.

The alternative would be to consider the forcing of dune soil cycles by fluctuations in the extreme wind regime that produces the dunes. At the base of the sedimentary sequence, the Mesolithic deposits are associated with more clayey layers with values two to three times higher than the overlying dune deposits. These layers correspond to the Mesolithic occupation surface on the aforementioned alterite layers, potentially associated or mixed with poorly developed loess. Here, blocks of rubified rock show magnetic susceptibility values up to 2.3 10^{-3} SI, i.e. almost double the values of the surface soil of the Mesolithic occupation, which is a marker of thermal alteration. In contrast, the bedrock reached in the test pits has values more than 10 times lower than the dune levels (<0.2 10^{-3} SI).

The three cycles of aeolian deposition and pedogenesis are clearly identifiable on the two extreme profiles. The dune part of the central profile appears to have much smoother and weaker values, as though there had been a mixture between the surface horizon, which is the least magnetic, and the underlying dune horizons. In the field, as we approach this central profile, the black horizons show a deepening and thinning, as though they correspond to the subsidence of the edges of a trench (fig. 18). The central magnetic susceptibility profile, therefore, seems to correspond to the filling of this trench.

Locally, very high magnetic susceptibility values (> 2 10-3 SI) were measured on the Mesolithic layers uncovered in one of the test pits. From an archaeological point of view, no hearth structures were observable. In view of the values seen on this level, in the vicinity or in the other test pit, such values can only be explained by thermo-alterations producing magnetic enhancement. The measurement of the magnetic susceptibility does not allow us to determine whether the thermo-altered material is still in its place in the hearth floor or whether it has since been displaced. To determine this, it would have been necessary to map the spatial variation of the magnetic field with the devices used in prehistoric caves (Burens et al., 2014; Grussenmeyer et al., 2014; Lévêque et Mathé, 2015). Such a mapping would have allowed either to identify a strong dipolar anomaly of the magnetic field, revealing the presence of a hearth, or the absence of such an anomaly, demonstrating that the high magnetic susceptibility recorded corresponds to hearth discharges. The absence of an archaeological structure identifiable as a hearth is not an argument for rejecting the hearth hypothesis. Such 'magnetic ghosts' are described in the literature (Linford, 2004; Schleifer, 2004; Simon et al., 2012).

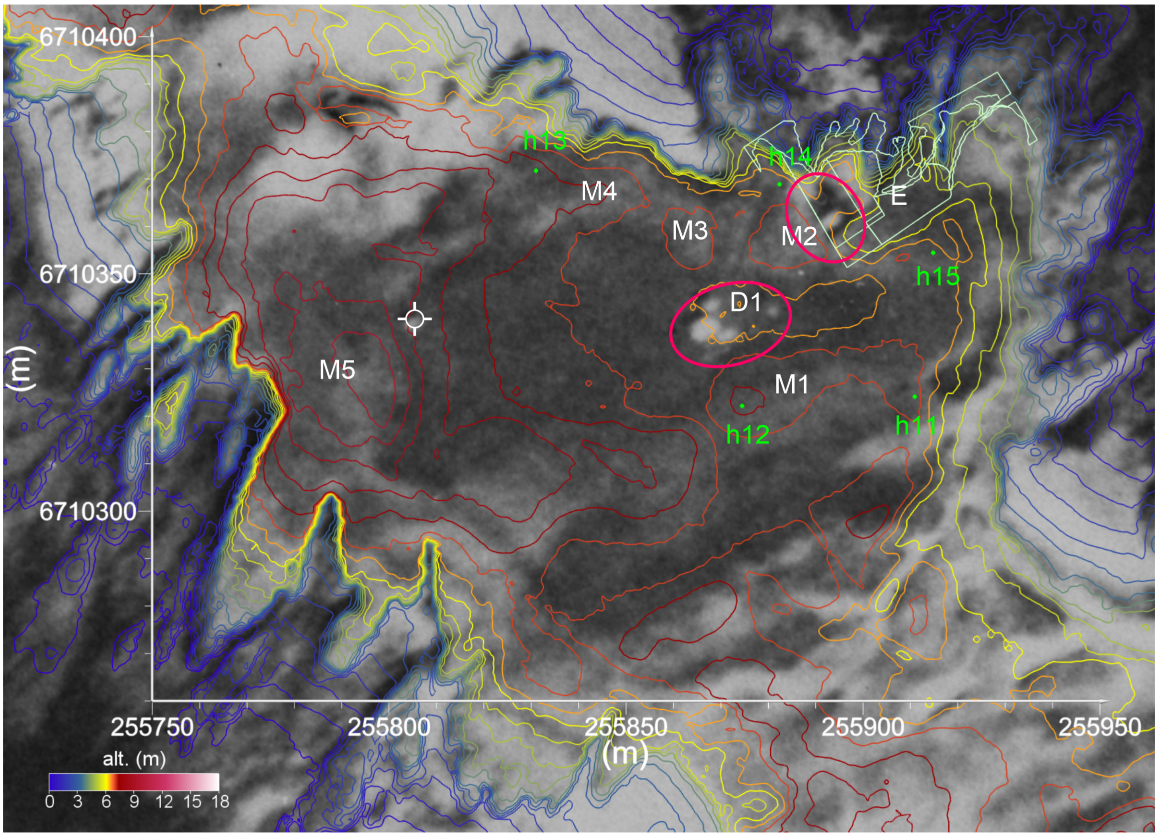

Fig. 17 – Position of the excavations carried out between 1931 and 1932 from an aerial view taken in August 1932. The 1932 image corresponds to the digitisation of a 1932 photograph negative (original IGN archive, Pierre Buttin's collection). The image is projected on a slightly slanted axis to reduce the distortion with respect to the 2019 orthophotograph. The presumed borders of the excavation are shown in green and the rock edges in light green (legend fig. 1).

***Fig. 17** – Localisation des fouilles réalisées entre 1931 et 1932 sur une vue aérienne prise en août 1932. L'image de 1932 correspond à la numérisation d'un contretype argentique d'une photographie de 1932 (original archive IGN, collection P. Buttin). L'image est projetée selon un axe légèrement incliné pour atténuer la distorsion par rapport à l'orthophotographie de 2019. Les limites présumées de la fouille sont figurées en vert et les limites des rochers, en vert clair (voir légende de la figure 1).*

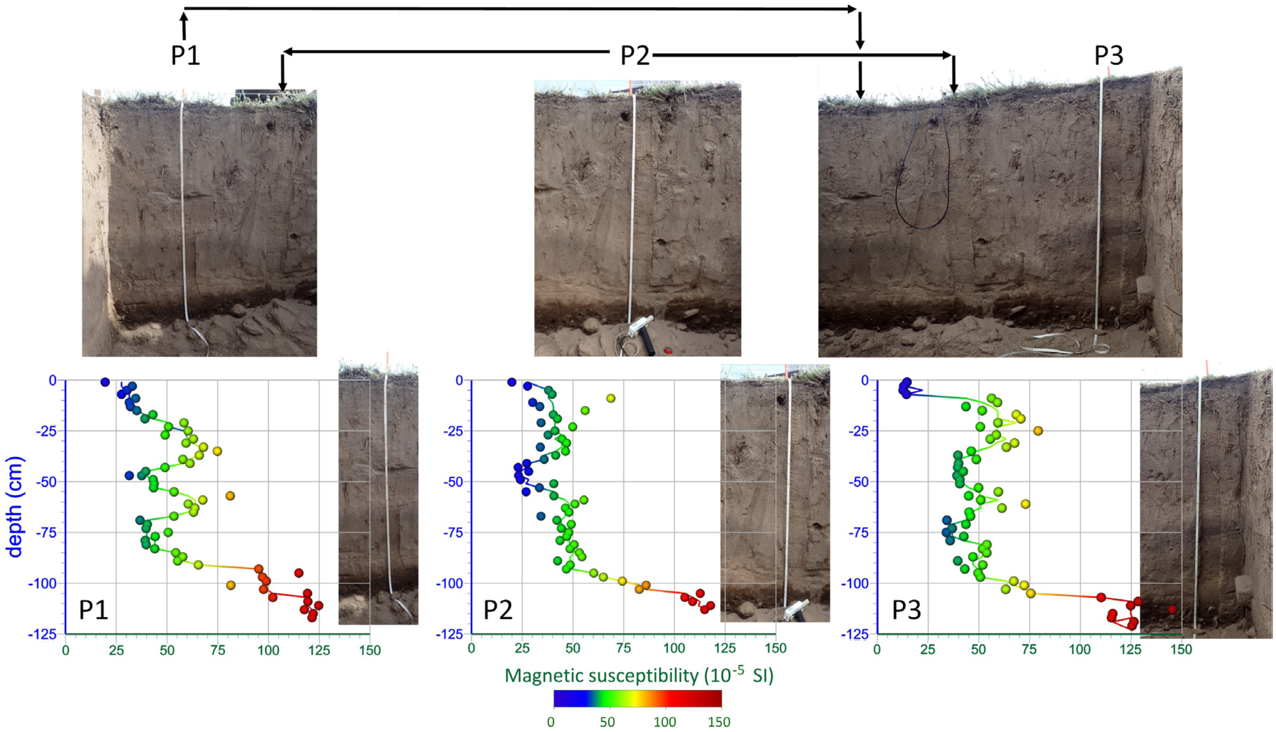

Fig. 18 – Magnetic susceptibility profiles in an archaeological test pit. Three magnetic susceptibility profiles taken less than a metre apart in the same pit. The information provided by the magnetic viscosity is similar and not shown. Profiles P1 and P3 show a similar signal. Profile P2 shows lower values in its upper part, indicating a mixture of materials from the less magnetic upper horizons. Thus, three levels of dune are identified, two capped by a paleosol and the last by a soil, showing a leaching of iron in the A horizon that implies low magnetic susceptibility values. Profile P2 seems to be located on a recent pit whose contours are difficult to identify.

***Fig. 18** – Profils de susceptibilité magnétique dans une fosse de sondage archéologique : trois profils réalisés à moins de 1 m d'intervalle dans une même fosse. L'information apportée par la viscosité magnétique est similaire et non présentée. Les profils P1 et P3 montrent un signal similaire. Le profil P2 présente des valeurs inférieures dans sa partie supérieure, attestant d'un mélange de matériaux issus des horizons supérieurs moins magnétiques. Ainsi trois niveaux de dune sont identifiés, chacun coiffé par un paléosol, ou sol pour le dernier, montrant un lessivage du fer dans l'horizon A, impliquant des valeurs de susceptibilité magnétique faibles. Le profil P2 paraît être situé sur une fosse récente dont les contours sont difficilement identifiables.*

This observation at the scale of a sondage shows the importance of observations made along vertical profiles, but also on the excavation surface. The data collected in this way completes the information obtained by the surface surveys. They allow a more in-depth interpretation of the data obtained on the surface, but also provide information that cannot be observed visually.

4. RECOMMENDATIONS FOR FUTURE STUDIES OF COASTAL SITES BY GEOMAGNETIC PROSPECTING

The purpose of this article is not to produce a plan for the use of geophysical or magnetic methods for geophysicists. It is rather to present them to archaeologists wishing to use them on their sites, to show how to proceed to obtain the best results possible. A part of this concerns what we could improve, or the instruments that could be developed to adapt our approaches to the problematic of the geophysical study of coastal archaeological sites, particularly to the detection of hearths.

4.1. Geopositioning

Given the unknowns about the intensity of the magnetic sources, their contrast with the surrounding materials and the depth of their burial, it is necessary to carry out a 'total field' survey (for geomagnetic field intensity), to be certain of being able to detect all potential sources. In addition, it is preferable to ensure the geopositioning of the measurements using a total station for laser-tracking. Indeed, the determination of the position of the spatial reference (antenna/reflector) can be increased from 1 per second using common GNSS up to 20 per second with the most powerful total stations. Accuracy also increases from a range of a few decimetres to centimetres using GNSS devices coupled to magnetometers to a range of centimetres or millimetres with a total station. The use of a miniature GNSS system with correction would allow centimetric geopositioning in planar space at rates that could reasonably reach five measurements per second. The vertical accuracy would remain lower than with a total station.

This 3D centimetric geopositioning will be all the more important as high spatial resolution 3D surveys will be implemented during excavation. Indeed, the integration of all the magnetic field intensity measurements into a common point cloud will require the precision of a total station.

To ensure repeatability of georeferencing, it is preferable to establish local reference points prior to any survey. If these points are to be within the survey area, non-magnetic materials such as brass, marine stainless steel (reference A4), wood or plastic should be used to mark them, so as not to disturb the magnetic signal.

4.2. Topography

It is preferable to plan the setting up of a survey to optimise the direction of the axis of the profiles to be covered so as to minimise variations in elevation (close to an East–West direction to minimise operator artefacts in geomagnetic prospecting). It is also preferable to foresee the placement positions of the total station to cover the entire target area, without masked areas. To prepare for these aspects, a digital terrain model (DTM) is required. In France, in the areas currently covered by Litto3D® coastal LiDAR surveys, a metric resolution DTM is available up to at least an altitude of 10 m and a distance of 2 km inland from the coast(1). For areas not covered, the RGE ALTI® 1m(2) provides similar information, but the altitude is only known to the decimetre whereas Litto3D® gives a centimetric accuracy. Artefacts do, however, appear in RGE ALTI®, in the connection zones between the different data sources used to build this model.

To obtain a more accurate elevation model, photographic coverage of the site can be made by drone, for example during the geophysical surveys. Photogrammetric processing of this coverage can then be used to obtain a digital elevation model (DEM) with sub-decimetric to centimetric spatial resolution depending on the flight parameters. Although a model with such a resolution is not necessary to define the implementation of geomagnetic prospection, in the future, the deliverables of a geomagnetic survey should correspond to a map of the sources and not of the anomalies they produce. For this, precise information on the microtopography must be integrated, requiring a DTM with centimetric resolution. Indeed, to obtain a geomagnetic signal with strong dynamics, it is necessary to be as close as possible to the source, i.e. to the ground surface. The microtopography generates a signal related to the contrast between the magnetic properties of the air and those of the ground. It is, therefore, necessary to take microtopography into account in future data processing algorithms for locating sources.

4.3. Apparatus

Similarly, the verticality error between the reflector and the sensors, linked to the failure to maintain the horizontality of the carried device during ascents or descents, generates spatialisation errors. These errors must be corrected to improve data quality. The change in incline can be determined from the change in altitude. However, this determination is not without uncertainty. Correcting this artefact at its source avoids the need to apply such an imperfect correction. To this end, a prototype carried device is being developed that will maintain the verticality between the reflector, the target of the laser tracking, and the magnetic field intensity measurement sensors. This new device will considerably reduce positioning errors linked to the problems of parallax deficiencies between the operator's perception of the relative position of the reflector in relation to the sensors and the horizontality of the device, which it is not always possible to maintain.

4.4. Complementary data

Improving the quality of the information provided should not only mean improving the geomagnetic survey protocols used or the processing of the data collected. It is also important to produce complementary data. Two types of complementary data can be distinguished. The first concerns the use of complementary geophysical imaging methods, which explore the environment based on properties of the ground other than magnetic properties. The second type of data results from a change of scale in the observation of magnetic properties, in contact with the archaeological layers after they have been exposed by excavation. Prior to the examination of these stratigraphic units, the collection of magnetic susceptibility measurements or high spatial resolution geomagnetic prospecting can provide information that is not visually observable, as a complement to the measurements carried out before stripping.

In the first of these types of data, the use of a conductivity meter shows the interest of observing the properties of the propagation of electrical currents. Depending on the nature of the remains, this property makes it possible to distinguish between clay enrichment (increase in electrical conductivity) or, on the contrary, stoniness (decrease in electrical conductivity). To increase the spatial resolution, but also to specify the depth of the variations observed, the electrical resistivity must be measured. This method is more complicated as it requires electrodes to be inserted into the ground. The distance between the electrodes determines the depth of investigation. Implemented along lines of electrodes or with fixed-distance electrodes mounted on a frame, this method allows either vertical profiles or maps to be made. If the electrical and magnetic property contrasts of the materials present are not correlated, then the information obtained will be complementary. Because of the relative speed of coverage of a surface with geomagnetic prospecting or with a conductivity meter, electrical methods are generally implemented on relevant sectors identified based on the information provided by the former. If the ground surface is sufficiently regular, then a ground-penetrating radar survey can be carried out. This will determine the presence of areas of abrupt material change, which are reflectors of the high frequency (hundreds of MHz) electromagnetic wave emitted.

Measuring apparent susceptibility with a conductivity meter provides a measurement of magnetic properties on a geomagnetic prospecting scale. By comparison with the geomagnetic information, its variation should, therefore, make it possible to determine the geomagnetic anomalies associated with sources carrying a strong remanent magnetisation, which is usually thermoremanent in archaeological contexts. Indeed, geomagnetic anomalies not associated with strong positive magnetic susceptibility anomalies are probably areas of strong thermoremanent magnetisation and, therefore, of a hearth still in place.

4.5 Nesting the scales of analysis

Moving from the scale of the site to that of the soil profile provides important information for understanding. Indeed, each soil has specific magnetic properties according to the dominant soil processes. The broad outlines of the dominant processes were described by the pioneer of the subject, E. Le Borgne (1955 and 1965). Since then, thanks to paleoclimatic studies of Quaternary loess, the role of rainfall has been identified. However, neither this last parameter nor those identified by E. Le Borgne can explain all the variability of the magnetic properties of the soils observed. In an area such as France, differences in rainfall are too small to be an explanatory factor. Therefore, our understanding is limited and, consequently, only observations using contact sensors can determine whether the soil is magnetically enhanced at the surface or, conversely, it is magnetically depleted in the organic horizon, as in the case of the dune soils presented. The two types of instruments to be preferred are susceptibility meters and magnetic viscometers. The former quantify an overall response of all soil constituents. Magnetic minerals, which have a very high susceptibility, are generally present in trace amounts. As a result, this quantity is strongly influenced by the relative content of the so-called non-magnetic minerals (diamagnetic: quartz, calcite, = slightly negative value; paramagnetic: ferromagnesian minerals, clays, = positive value). Magnetic viscosity has the advantage of being independent of these non-magnetic minerals since it only looks at the unstable part of the remanent magnetisation borne by ferromagnetic minerals, in the broad sense, of nanometric size, called superparamagnetic. This nanometric phase is classically produced by pedogenesis or by thermo-alteration. By comparing different soil profiles, the joint observation of the variations of these two quantities makes it possible to determine the materials showing a magnetic enhancement that may be associated with thermo-alteration processes from those more likely to be of pedological origin, based on the differences in signatures observed.

These soil profiles can be accessed either by coring or archaeological test pits. Coastal erosion has also provided access to profiles in the vicinity of the target site, allowing easy examination of the spatial variability of the magnetic signature of the surface cover. Such measurements can also be made during an excavation. The presence of a geophysicist during a whole excavation does not appear to be the best solution. Similarly, the production of a susceptibility or magnetic viscosity variation map is laborious. Consequently, it is necessary for the excavator to become familiar with the use of these instruments. A phase of analysis to understand the sources of variability of magnetic susceptibility and viscosity must be conducted by a geophysicist. Then, once the geophysicist has defined the protocol, it will be up to the excavator to make the measurements. However, this approach does not allow the detection of magnetic ghosts, i.e. hearth floors leaving no significant visible trace.

One solution is to carry out geomagnetic surveys with sub-decimetric spatial resolution, similar to what is done in prehistoric caves (Burens et al., 2014; Grussenmeyer et al., 2014; Lévêque et Mathé, 2015; Jaubert et al., 2016). Necessarily, due to the attenuation of the signal with distance, these surveys must be done in contact with the archaeological layer. This implies that the targeted archaeological surface must be cleared over a significant area in order to obtain an image of exploitable space. The use of iron pegs for the archaeological grid is, therefore, not recommended. Instead of the commonly used metal nails, plastic or wooden equipment should be used. It is also necessary to allow for the time needed to carry out the prospection in the absence of any moving metal object or other source of magnetic disturbance meaning that a halt in excavation activities would be necessary. Finally, once the image of the magnetic field variation has been obtained, it is necessary to go back over the site to identify the origin of the anomalies observed by means of magnetic susceptibility measurements.

Because of the need for a spatialised measurement to obtain an image, this approach, although very informative, requires complex instrumentation. An alternative to this approach would be to proceed as for the detection of networks in public works, through the identification of anomalies by the detection of extreme values. This would require an instrument that is quick to use on the excavation site without requiring interruption of the excavation. An instrument is, therefore, needed that determines strong spatial variations in the magnetic field over short distances so that variations induced by disturbances produced a few metres away by other excavators are not detectable. Such a signal can be obtained with a device that determines the differences in magnetic field strength over a short distance. For the signal to remain detectable, a distance of a few decimetres is required. Such a gradiometer does not yet exist but seems easy to design.

In the presence of burnt or rubified materials, the excavator could search for the presence of a hearth by looking for zones of magnetic enhancement with the susceptibility meter or viscometer. If they identify such a zone, then they can then locate the hearth by looking for magnetic field gradient peaks. At our latitude, the hearth should be approximately halfway between the positive and negative peaks. If no significant magnetic field anomaly is detected at the level of the magnetic enhancement zone, then this means that a hearth emptying zone is present.

This shows that geophysical investigations can also be carried out during an excavation. The archaeological observations made during the excavation must also be cross-referenced with the geophysical information (this work remains to be done in the case of the test pits at Port Neuf). The interest is to compare the geophysical interpretations with the reality of the field. In case of discrepancy, the new data will allow us to identify the interpretation error and explain its origin. The geophysicist, therefore, acquires new experience that will allow them to adapt their investigation protocol for the study of another similar site. The interpretation of their data will be improved and thus better guide archaeological excavations on new sites. Open areas can be limited and areas not yet in danger of erosion will be preserved.

The geophysicist's interpretation is based on the spatial coherence of the nature of the physical contrasts observed. However, the study of a site cannot be limited to a geophysical study as this cannot provide chronological data. Archaeological excavation provides stratigraphic information that is otherwise inaccessible. Geophysics makes it possible to widen the area of investigation and to place an excavation in its context. For this reason, it is important that the geophysicist carries out their surveys before any test pit is made. Indeed, a test pit brings about modifications of the spatial variation of the physical properties of the environment. It is, therefore, important that archaeologists and geophysicists work together.

Acknowledgement: This publication work is supported by funding from the French National Research Agency (ANR-21-CE27-0024) and the program "Actuaciones Arqueologicas en el Exterior" of the Spanish Ministry of Culture for IIIPC, Santander, Universidad de Cantabriar.
The geophysical equipment used was funded by the "Contrats de Plan État-Région Poitou-Charentes" 2007-2014 and 2015-2020.
The digitization of the countertype of the aerial photograph of 1932 (31e RAO Esc. 15 19-8-32 Rec no. 3, cl no. 10, collection Pierre Butin) was carried out by Philippe Lévêque on a scanner V850 (Epson) of the photography section of the lycée professionnel Victor-Laloux, 6 avenue Monge, 37200 Tours, France.

NOTES

(1) https://services.data.shom.fr/static/specifications/DC_Litto3D.pdf
(2) https://geoservices.ign.fr/rgealti

BIBLIOGRAPHY

Bates C. R., Bates M., Gaffney C., Gaffney V., Raub T. D. (2019) – Geophysical Investigation of the Neolithic Calanais Landscape, *Remote Sensing*, 11, 24, p. 2975, https://doi.org/10.3390/rs11242975

Brodard A., Guibert P., Lévêque F., Mathé V., Burens A., Carozza L. (2014) – Thermal Characterisation of Bronze Age Hearths from the Cave of Les Fraux (Dordogne, France) by Thermoluminescence and Magnetic Susceptibility Techniques, in R. H. Tykot (ed.), *From Bioarchaeology to Integrated Site Studies*, proceedings of the 38th International Symposium on Archaeometry (Tampa, Florida, May 10th-14th 2010), *Open Journal of Archaeometry*, 2, 5457, https://doi.org/10.4081/arc.2014.5457

Brodard A., Lacanette-Puyo D., Guibert P., Lévêque F., Burens A., Carozza L. (2016) – A New Process of Reconstructing Archaeological Fires from their Impact on Sediment: A Coupled Experimental and Numerical Approach Based on the Case Study of Hearths from the Cave of Les Fraux (Dordogne, France), *Archaeological Anthropological Sciences*, 8, p. 673-687, https://doi.org/10.1007/s12520-015-0250-7

Burens A., Grussenmeyer P., Carozza L., Lévêque F., Guillemin S., Mathé V. (2014) – Benefits of an Accurate 3D Documentation in Understanding the Status of the Bronze Age Heritage Cave "Les Fraux" (France), *International Journal of Heritage in the Digital Era*, 3, 1, p. 179-195, https://doi.org/10.1260/2047-4970.3.1.179

Colombo U., Gazzarrini F., Lanzavecchia G. (1967) – Mechanisms of Iron Oxides Reduction at Temperatures Below 400 °C, *Materials Science and Engineering*, 2, p. 125-135, https://doi.org/10.1016/0025-5416(67)90030-4

Cousseau F., Cassen S., Daire M.-Y., Duval H., Gouézin P., Grimaud V., Guiavarc'h M., Lévêque F., Matin C., Querré G. (2019) – *Architectures et technologies des tumulus néolithiques bretons* : *la nécropole de Guennoc à Landéda (Finistère)*, rapport de prospection thématique 2017-2018, RAP03676, service régional de l'archéologie Bretagne, Rennes, 194 p.

Cudennec Y., Lecerf A. (2005) – Topotactic Transformations of Goethite and Lepidocrocite into Hematite and Maghemite, *Solid State Science,* 7, 5, p. 520-529, https://doi.org/10.1016/j.solidstatesciences.2005.02.002.

Duval H., Peres T., Lévêque F., Mathé V., Collado E. (2021) – Nouvelles acquisitions sur le site de Coh-Castel à Belle-Île-en-Mer (Morbihan), in F. Delrieu, C. Féliu, P. Gruat, M.-C. Kurzaj and É. Nectoux (eds.), *Les espaces fortifiés à l'âge du Fer en Europe*, actes du 43e colloque international de l'AFEAF, (Le Puy-en-Velay, 30 mai-1er juin 2019), Paris, Association française pour l'étude de l'âge du Fer, p. 247-252.

Fassbinder J. W. E. (2015) – Seeing Beneath the Farmland, Steppe and Desert Soil: Magnetic Prospecting and

Soil Magnetism, *Journal of Archaeological Science*, 56, p. 85-95, https://doi.org/10.1016/j.jas.2015.02.023.

Giovas C. M., Kappers M., Lowe K. M., Termes L. (2020) – The Carriacou Ecodynamics Archaeology Project: First Results of Geophysical Survey and Landscape Archaeology at the Sabazan Site, The Grenadines, *The Journal of Island and Coastal Archaeology*, 15, 3, p. 421-435, https://doi.org/10.1080/15564894.2019.1642969

Grussenmeyer P., Burens A., Carozza L., Lévêque F., Guillemin S., Mathé V. (2014) – Numérisation 3D de la grotte ornée des Fraux (Dordogne) : apport à l'archéologie et à la cartographie du champ magnétique, *Revue de l'Association française de topographie*, 138, 1[er] trimestre 2014, p. 33-41.

Jaubert J., Verheyden S., Genty D., Soulier M., Cheng H., Blamart D., Burlet C., Camus H., Delaby S., Deldicque D., Edwards R. L., Ferrier C., Lacrampe-Cuyaubère F., Lévêque F., Maksud F., Mora P., Muth X., Régnier É., Rouzaud J.-N., Santos F. (2016) – Early Neanderthal Constructions Deep in Bruniquel Cave in Southwestern France, *Nature*, 534, p. 111-114, https://doi.org/10.1038/nature18291

Le Borgne E. (1955) – Susceptibilité magnétique anormale du sol superficiel, *Annales de* géophysique, 11, p. 399-419.

Le Borgne E. (1965) – Les propriétés magnétiques du sol. Application à la prospection des sites archéologiques, *Archaeo-physika*, 1, p. 1-20.

Lecoanet H., Lévêque F., Segura S. (1999) – Magnetic Susceptibility in Environmental Applications: Comparison of Field Probes, *Physics of the Earth and Planetary Interiors*, 115, 3-4, p. 191-204, https://doi.org/10.1016/S0031-9201(99)00066-7

Lévêque F. (2021) – Magnetic properties of soils, in G. Odonne and J.-F. Molino (eds.) *Methods in Historical Ecology: Insights from Amazonia*, London/New York, Routledge, 185 p.

Lévêque F., Mathé V. (2015) – Prospection magnétique 3D à haute résolution. Du site à l'objet, *Les Nouvelles de l'archéologie*, 138, p. 19-23, https://doi.org/10.4000/nda.2697

Linford N. T. (2004) – Magnetic Ghosts: Mineral Magnetic Measurements on Roman and Anglo-Saxon Graves, *Archaeological Prospection*, 11, p. 167-180, https://DOI.org/10.1002/arp.232

Maher B. A. (2011) – The Magnetic Properties of Quaternary Aeolian Dusts and Sediments, and their Palaeoclimatic Significance, *Aeolian Research*, 3, 2, p. 87-144, https://doi.org/10.1016/j.aeolia.2011.01.005

Menier D., Reynaud J.-Y., Proust J.-N., Guillocheau F., Guennoc P., Bonnet S., Tessier B., Goubert E. (2006) – Basement Control on Shaping and Infilling of Valleys Incised at the Southern Coast of Brittany, France, in R. W. Dalrymple, D. A. Leckie and R. W. Tillman (eds), *Incised Valleys in Time and Space*, Tulsa, Society for Sedimentary Geology, 85, p. 37-55, https://doi.org/10.2110/pec.06.85.0037.

Menier D., Scalliet F., Proust J.-N., Cassen S. (2009) – Contexte géomorphologique et paléoenvironnemental en Bretagne sud au Pléistocène, in S. Cassen (ed.) *Autour de la table. Explorations archéologiques et discours savants sur des architectures néolithiques à Locmariaquer, Morbihan. (Table des Marchands et Grand Menhir)*, Nantes, Lara-université de Nantes, p. 800-813.

Napora K. G., Bonsall J., Rathbone S. D., Thompson V. D. (2019) – Geoarchaeological Analysis of a Dunefield Shell Midden Site in Carrowdough Townland, County Sligo, Ireland, *The Journal of Island and Coastal Archaeology*, 14, p. 394–410, https://doi.org/10.1080/15564894.2018.1531332.

Pailler Y., Nicolas C., Corsi L., Dréano Y., Jézéquel M., Le Bris D., Lévêque F., Manceau L., Paillard C., Stéphan P., Paulet Y.-M., Prévost C., Villagran X. (2022) – Première campagne de fouille programmée sur le site multi-périodes de Porz ar Puns, île de Béniguet (Le Conquet, Finistère), excavation report, Service régional de l'archéologie Bretagne, Rennes, p. 198.

Péquart M., Péquart S.-J. (1929) – La nécropole mésolithique de Téviec (Morbihan) : Nouvelles découvertes, *L'Anthropologie*, 38, p. 373-400.

Péquart M., Péquart S.-J. (1954) – Hoëdic, deuxième station-nécropole du Mésolithique côtier armoricain, Anvers, De Sikkel, 93 p.

Rgealti (2018) – Référentiel à grande échelle altimétrique RGE ALTI®, IGN, BDALTIV2_MNT_250M_ASC_LAMB93_IGN69_FRANCE, traitement 2018.

Rgealti (2021) – Référentiel à grande échelle altimétrique RGE ALTI®, IGN, IGNF_RGEALTIr_2-0_ASC_1M_LAMB93_IGN69_D056_20211003, traitement du 2021-10-03

Schleifer N. (2004) – Ghost features. A Proposal for Appropriate Management and a Forum for Discussion, *ISAP News*, 1, p. 6-9.

Shom (2015a) – MNT Bathymétrique de la façade Atlantique (Projet Homonim), http://www.shom.fr/BATHYMETRIE/ServiceMNT_ATL100m_HOMONIM_WGS84

Shom (2015b) – MNT topo-bathymétrique côtier de la zone « Morbihan » à 20 m (Projet TANDEM), http://dx.doi.org/10.17183/MNT_COTIER_MORBIHAN_TANDEM_20m_WGS84

Simon F.-X., Koziol A., Thiesson J. (2012) – Investigating Magnetic Ghosts on an Early Middle Age Settlement: Comparison of Data from Stripped and Non-Stripped Areas, *Archaeological Prospection*, 19, p. 191-200, https://doi.org/10.1002/arp.1427

Tite M.S., Mullins C. (1971) – Enhancement of the Magnetic Susceptibility of Soils on Archaeological Site, *Archaeometry*, 13, 2, p. 209−219, https://doi.org/10.1111/j.1475-4754.1971.tb00043.x

Wilken D., Hadler H., Wunderlich T., Majchczack B., Schwardt M., Fediuk A., Fischer P., Willershäuser T., Klooss S., Vött A., Rabbel W. (2022) – Lost in the North Sea. Geophysical and Geoarchaeological Prospection of the Rungholt Medieval Dyke System (North Frisia, Germany), *PLoS ONE*, 17, 4, e0265463, https://doi.org/10.1371/journal.pone.0265463

Yu J., Han Y., Li Y., Gao P., Li W. (2017) – Mechanism and Kinetics of the Reduction of Hematite to Magnetite with CO-CO_2 in a Micro-Fluidized Bed, *Minerals*, 7, 11, p. 209, https://doi.org/10.3390/min7110209

François Lévêque
LIENSs UMRi 7266
CNRS - La Rochelle Université
La Rochelle, France
francois.leveque@univ-lr.fr

Grégor Marchand (†)
CNRS UMR 6566 CReAAH
Université de Rennes
Rennes, France
gregor.marchand@univ-rennes1.fr

Martin Moucheron
School of Archaeology
University College Dublin
Dublin, Ireland
martin.moucheron@ucdconnect.ie

Luis Teira
IIIPC, Universidad de Cantabria
Santander, Spain
luis.teira@unican.es

Pablo Arias
IIIPC, Universidad de Cantabria
Santander, Spain
pablo.arias@unican.es